Supporting Information
For the
Manuscript

Sulfur-hinged L-shaped ligand-based Cd(II)-organic framework: A fluorescent tool for targeting environmental nitroaromatics†

Nitu Rani,[a] Aman K. K. Bhasin,[b] Ahamd Husain,[c] Annu Kumari, [d] Reshu Verma,[d] K. K. Bhasin*[a] and Girijesh Kumar*[d]

[a]*Department of Chemistry & Centre for Advanced Studies in Chemistry, Panjab University, Chandigarh-160014, India*

[b]*Department of Chemistry, DAV University Jalandhar, Punjab-144012, India*

[c]*Department of Chemistry, Amity University, Sector 82A, Mohali, Punjab-140306, India*

[d]*Department of Chemistry, University of Allahabad, Prayagraj, Uttar Pradesh-211002, India.*

Email: girijeshkumar@allduniv.ac.in, girijeshchem@gmail.com

Synthesis of ligand N, N'-(thiobis(4,1-phenylene)) diisonicotinamide (L$^{4\text{-py}}$).[S1] The ligand **L$^{4\text{-py}}$** has been synthesized using isonicotinic acid (0.227 g, 0.92 mmol) and 4,4'-thiodianiline (0.100 g, 0.46 mmol) which were dissolved in pyridine (3 mL) and heated at 90 °C for 40 min (Scheme S1). After heating the solution triphenylphosphite (TPP) (0.241 mL, 0.92 mmol) was added drop wise and the reaction was stirred for 8 h. The progress of the reaction was monitored by thin-layer chromatography (TLC). After completion of the reaction, ice-cold water was added to it and an off-white solid precipitated out filtered off and was washed with cold water several times followed by diethyl ether. The precipitates were dried at 60 °C for 12 h in an oven. Yield (0.180 g, 91 %; based on 4,4'-thiodianiline). FT-IR spectrum (selected peaks; ν cm^{-1}): 3288 (N-H), 1647, 1590 (C=O$_{amide}$). ^{1}H NMR (500 MHz, DMSO-d_6); δ_{ppm} 7.35-7.37 (*d,* 4H, *J* = 8.7 Hz, H$_a$), 7.85-7.86 (*d,* 4H, *J* = 6.0 Hz, H$_b$), 7.80-7.81 (*d,* 4H, *J* = 8.7 Hz, H$_c$), 8.78-8.80 (*d,* 4H, *J* = 5.9 Hz, H$_d$), 10.60 (*s,* 2H, He). ^{13}C NMR (126 MHz, DMSO-d_6) δ_{ppm} 163.96, 150.17, 141.64, 137.93, 131.26, 129.88, 121.45, 121.24.

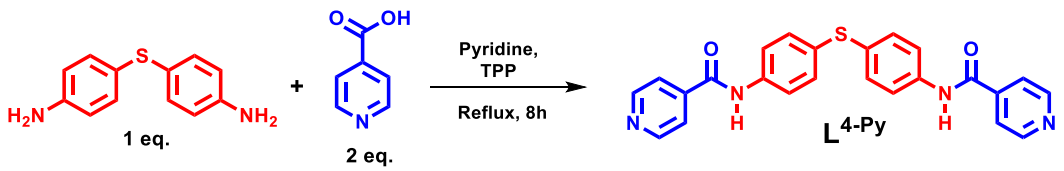

Scheme S1. Synthesis of ligand N, N'-(thiobis(4,1-phenylene)) diisonicotinamide (**L$^{4\text{-py}}$**).

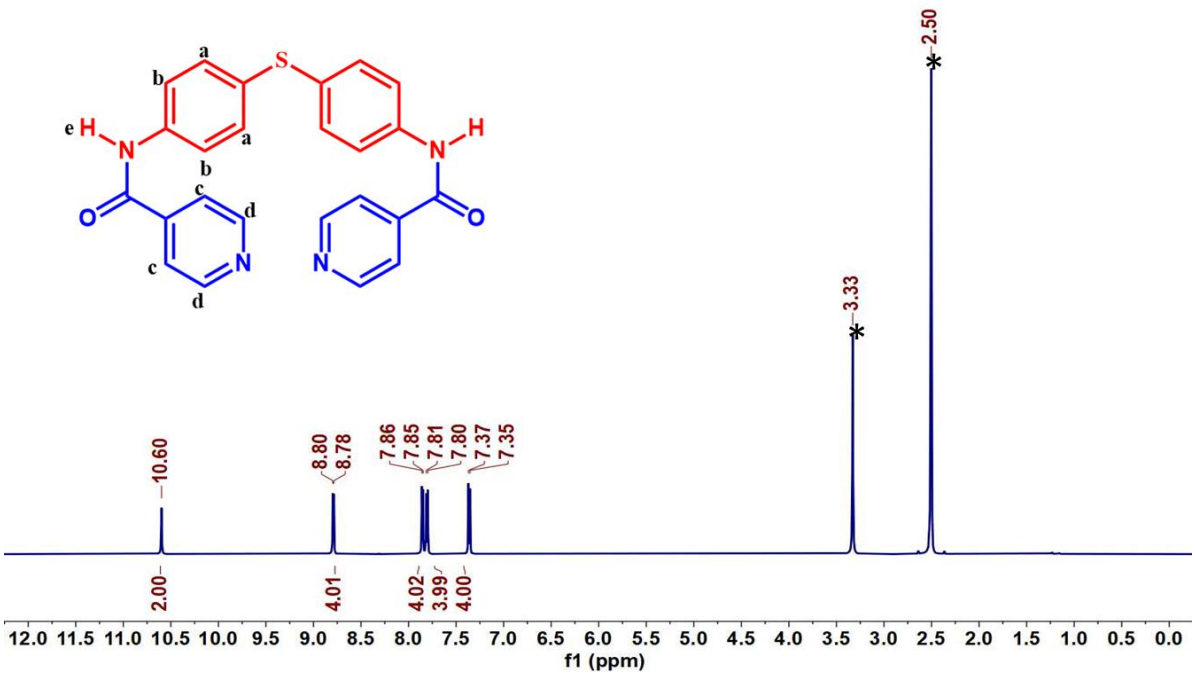

Fig. S1. ^{1}H NMR spectrum of ligand **L$^{4\text{-py}}$** in DMSO-d_6. *Represents the residual water peak is at 3.33 ppm.

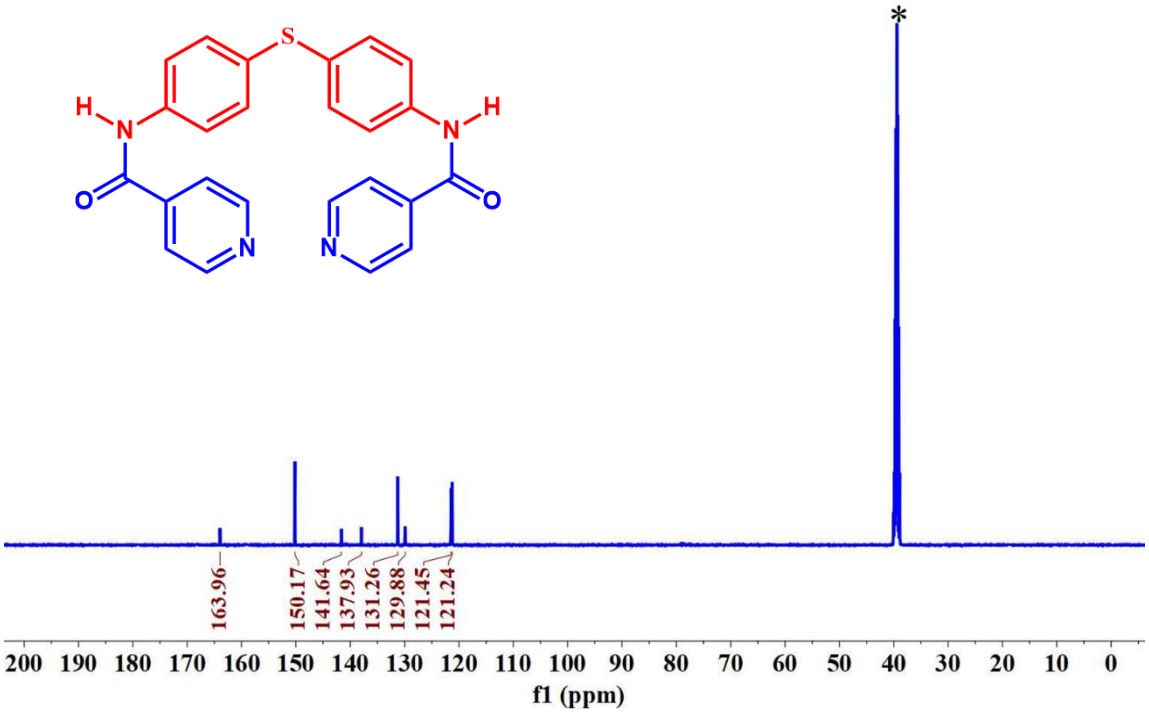

Fig. S2. ^{13}C NMR spectrum of ligand **L$^{4\text{-py}}$** in DMSO-d_6. *Represents the solvent residual peak.

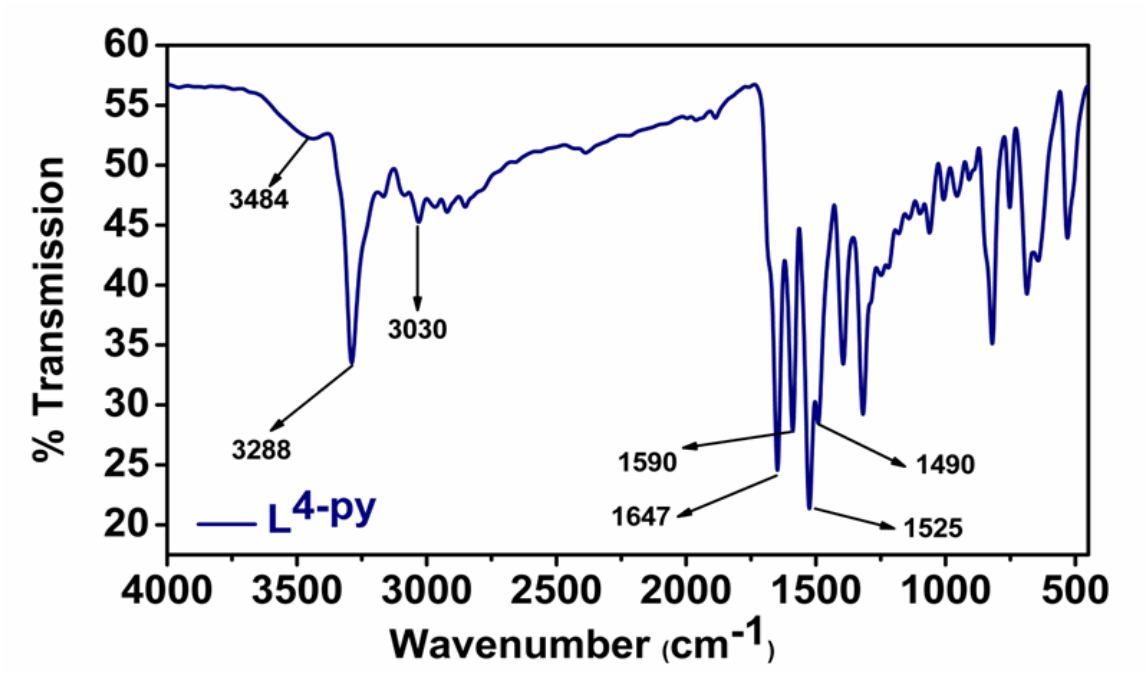

Fig. S3. FT-IR spectrum of ligand **L$^{4\text{-py}}$**.

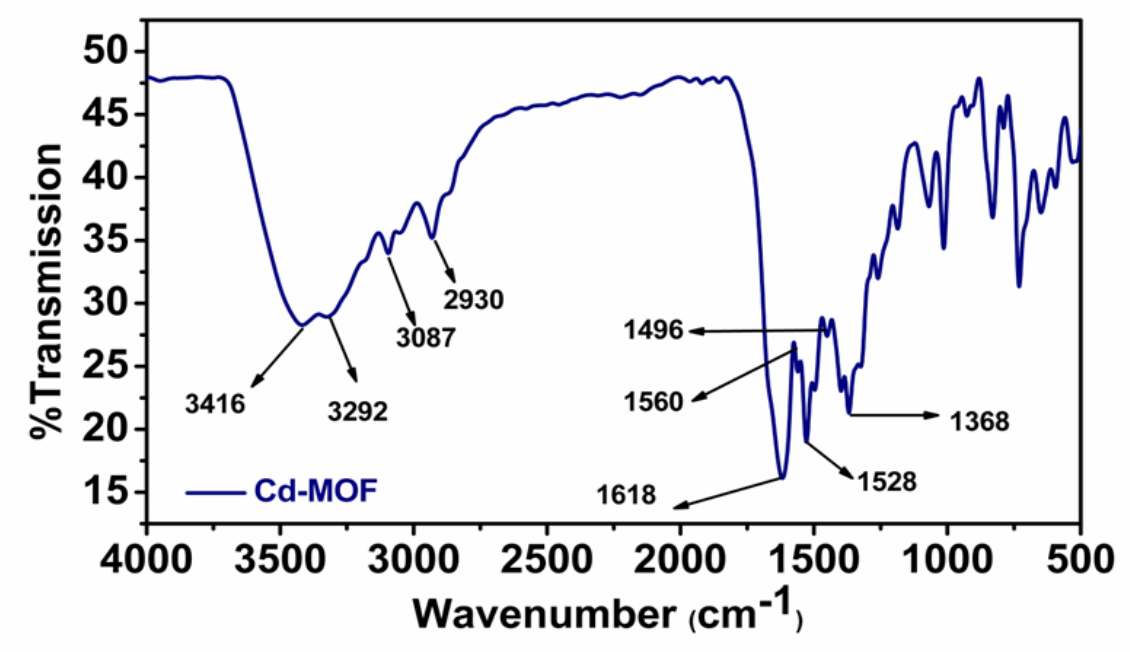

Fig. S4. FT-IR spectrum of **Cd-MOF**.

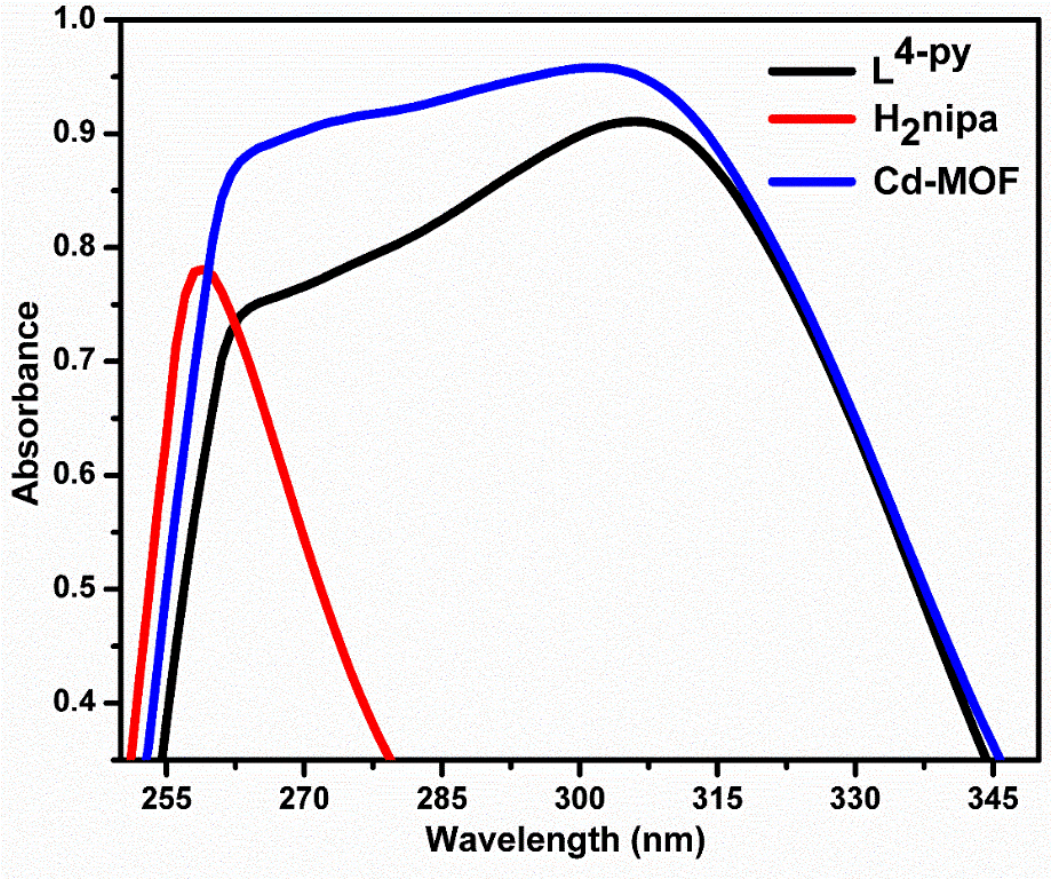

Fig. S5. UV-Visible spectra of ligand **$L^{4\text{-py}}$**, co-ligand H_2nipa and **Cd-MOF** in DMSO.

Deptt. of CIL , Panjab University Chandigarh

Company name:	**ThermoFinnigan**
Analysed:	**15-07-2024 14:10**
Printed:	**19-12-2024 15:03**
Sample ID:	**Cd-MOF**
Analysis type:	**UnkNown**
Chromatogram filename:	**C:\CHNS-O\SAIF\CHNS\User 2024\July\15-7-2024\8.DAT**
Calibration method:	**K Factors**
Sample weight:	**2.369**

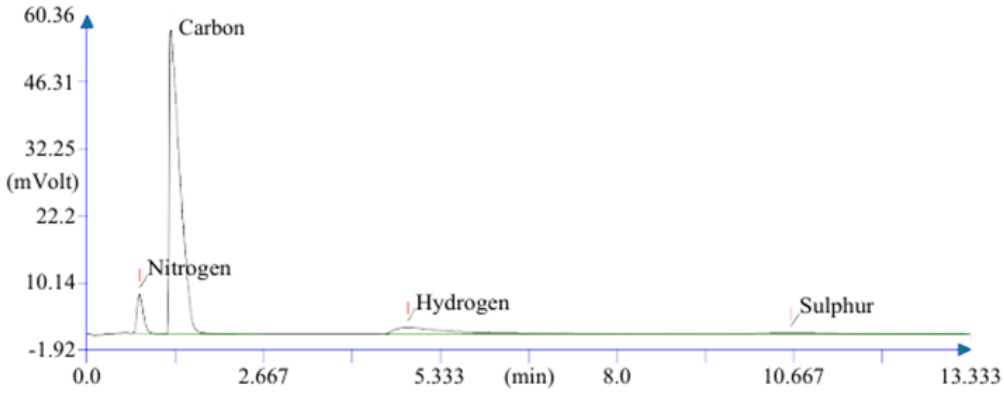

Peak Number (#)	Retent(ion Time min)	Component Name	Element %
1	0.800	Nitrogen	9.013
2	1.267	Carbon	51.01
3	4.842	Hydrogen	4.151
4	10.625	Sulphur	3.336
			67.51

Fig. S6. CHNS data of **Cd-MOF.**

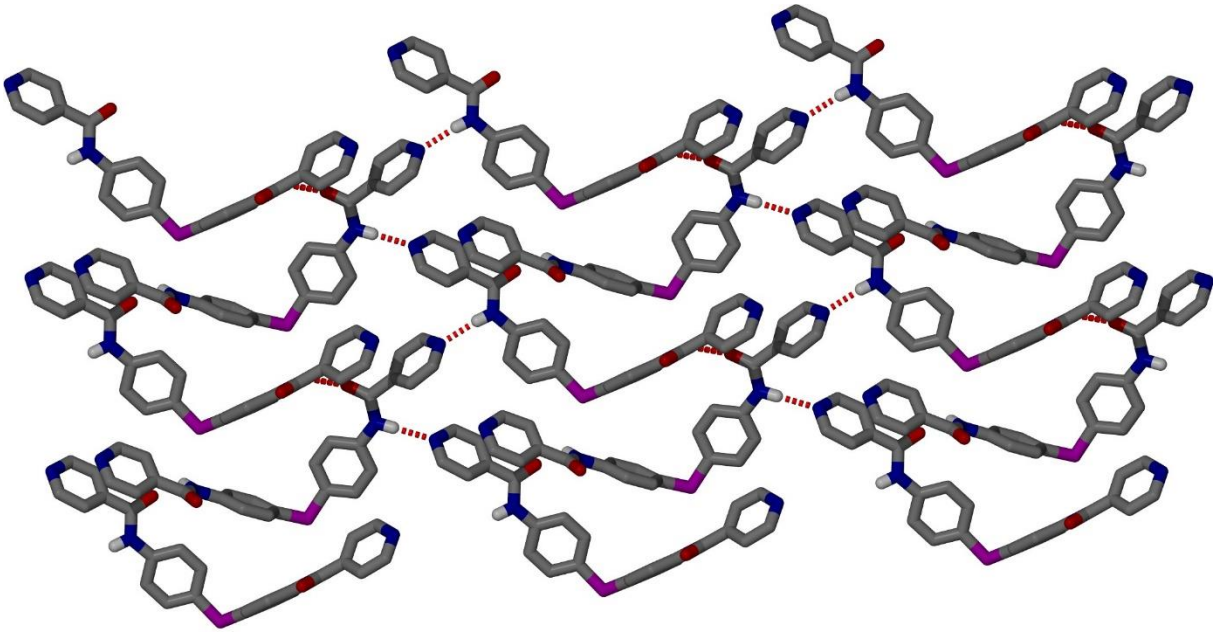

Fig. S7. H-bonding interactions involving N–H---N and N–H---O of amide functionalities of **L**$^{4\text{-Py}}$.

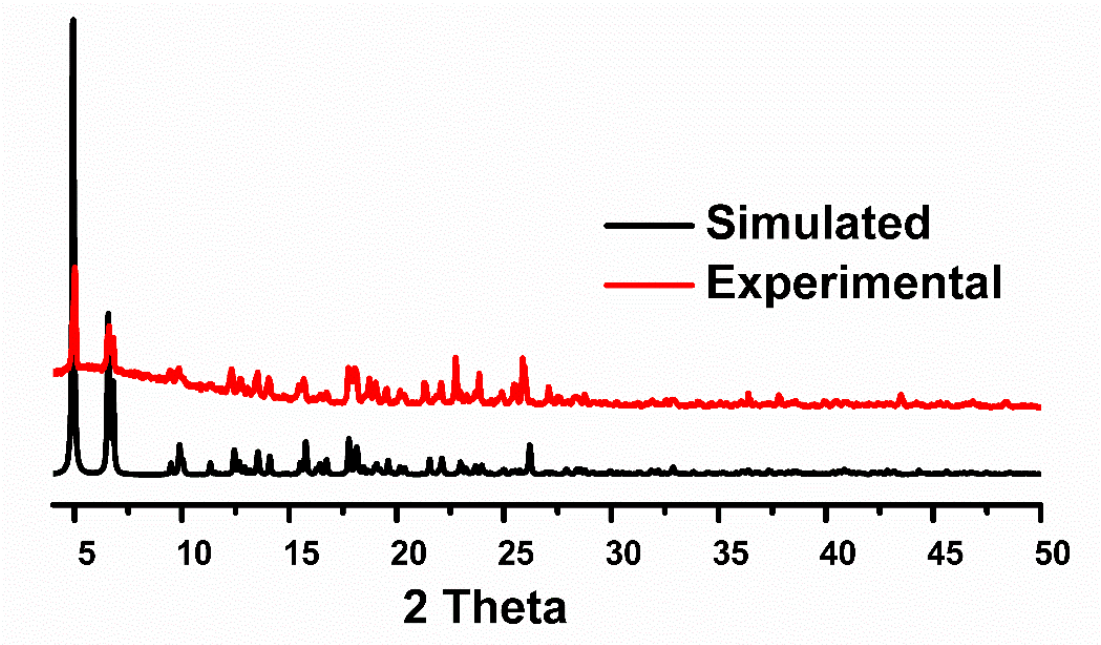

Fig. S8. PXRD pattern for **Cd-MOF** bulk sample (red trace) and the one simulated from the single crystal structure analysis (black trace)**.**

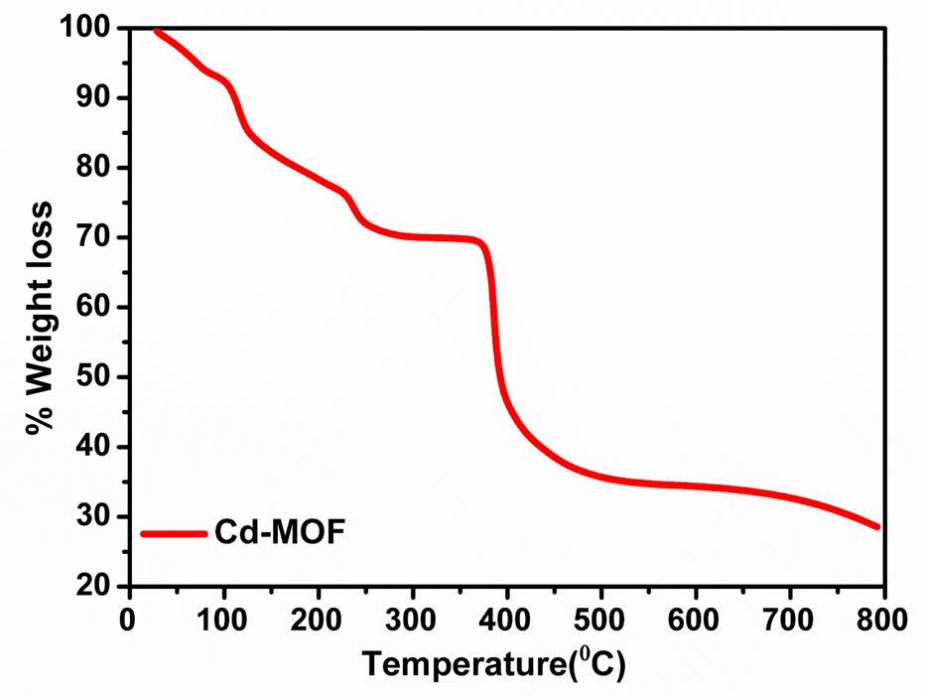

Fig. S9. TGA plot for **Cd-MOF**.

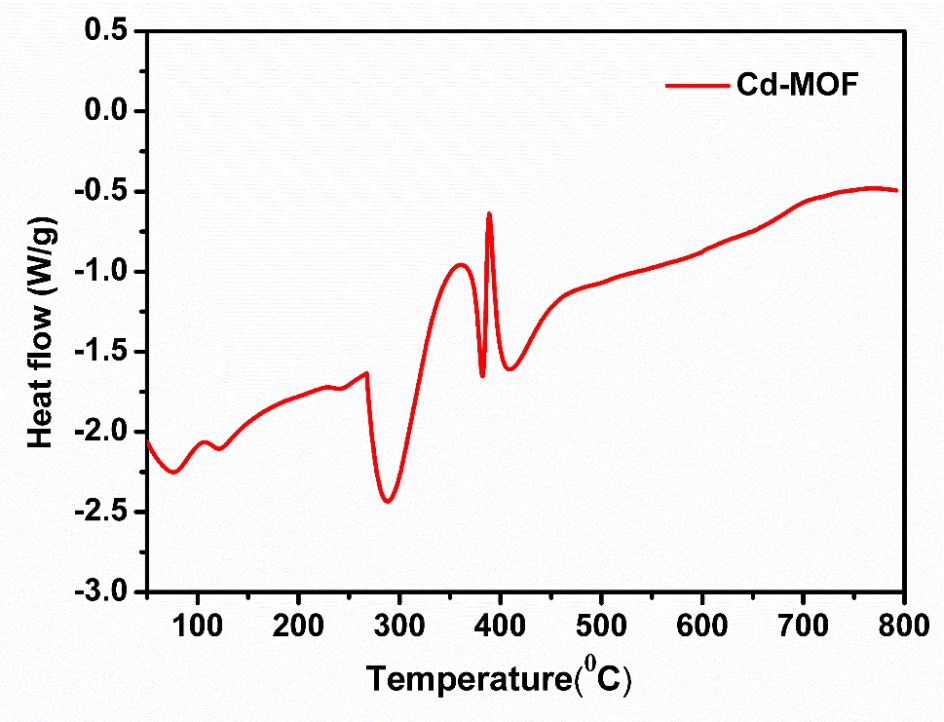

Fig. S10. DSC plot for **Cd-MOF.**

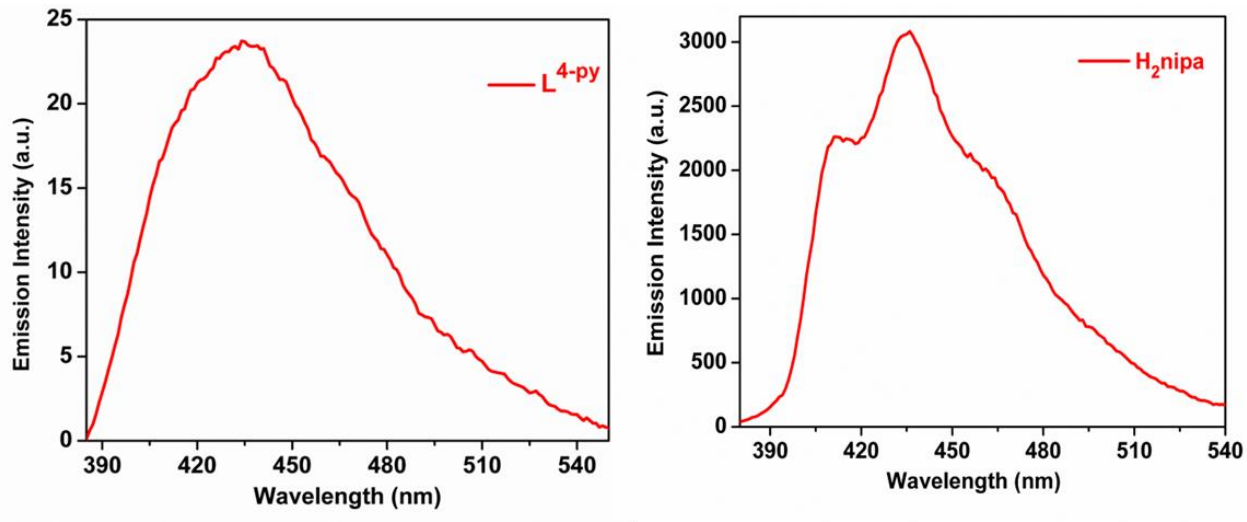

Fig. S11. Emission spectra of (a) **$L^{4\text{-py}}$** and (b) co-ligand H_2nipa.

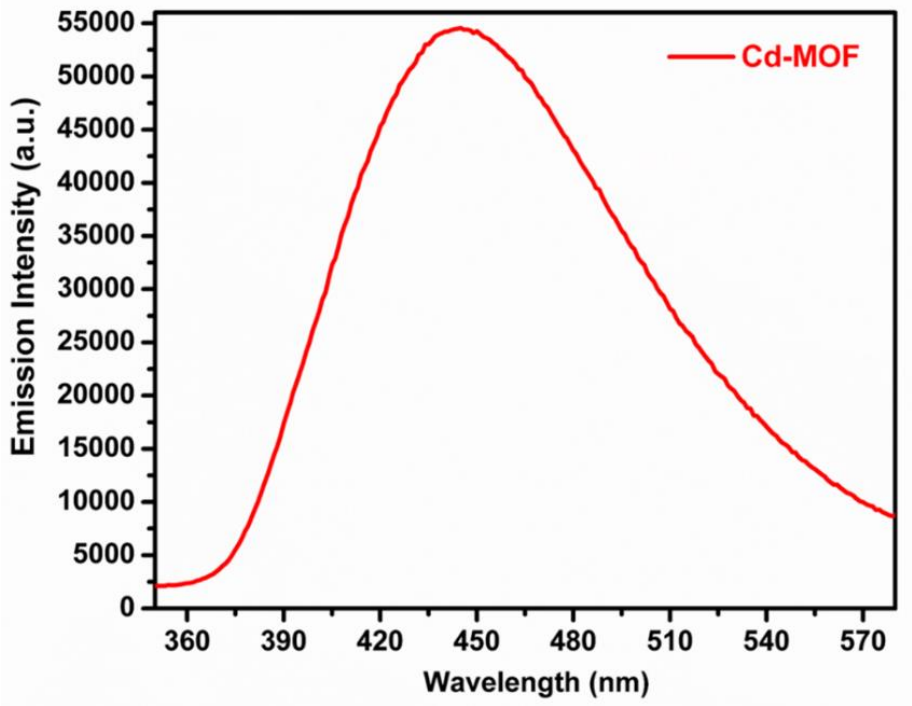

Fig. S12. Emission spectra **Cd-MOF**.

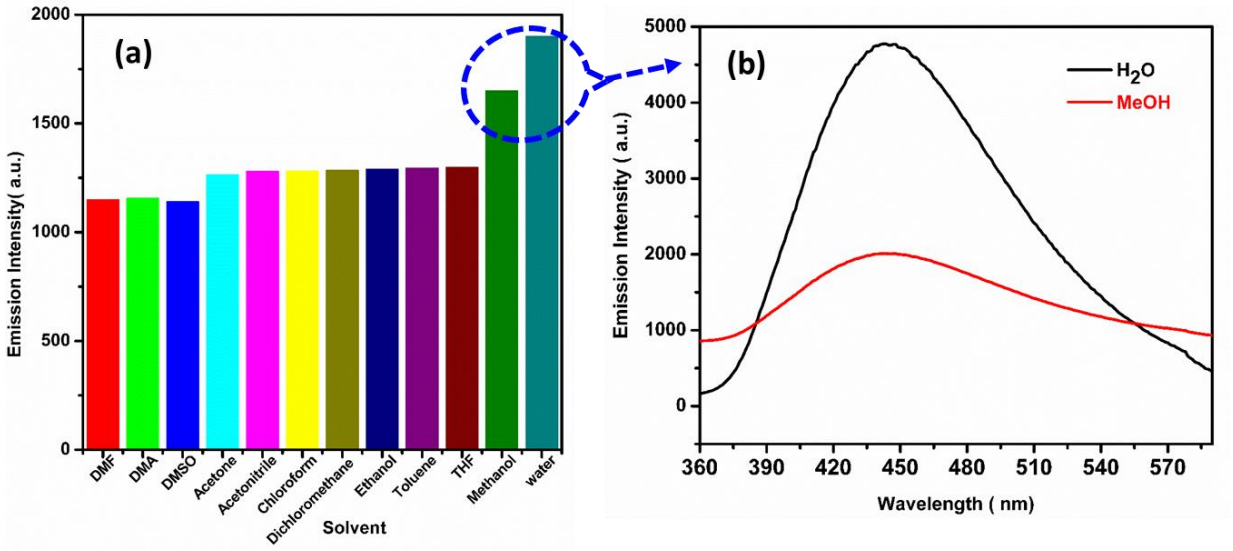

Fig. S13. (a) Emission Profile of **Cd-MOF** in different solvents. (b) Emission Profile of **Cd-MOF** in H_2O and dry MeOH, wherein the highest emission intensity observed.

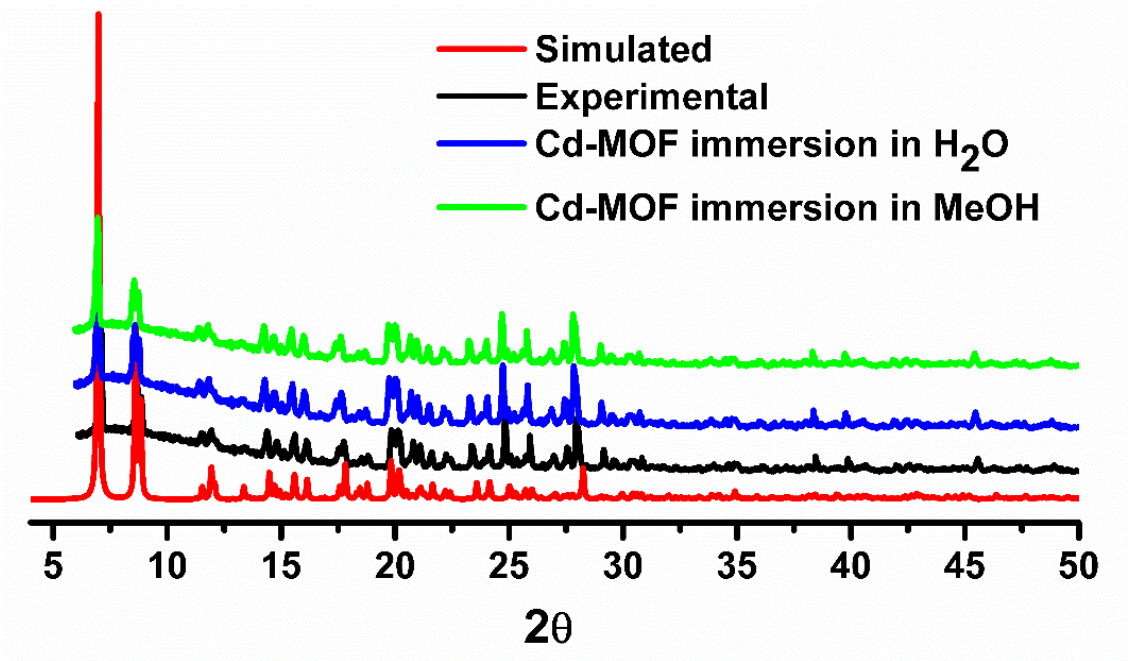

Fig. S14. PXRD pattern of **Cd-MOF** and the samples recovered after soaking in H_2O and MeOH for 24 h.

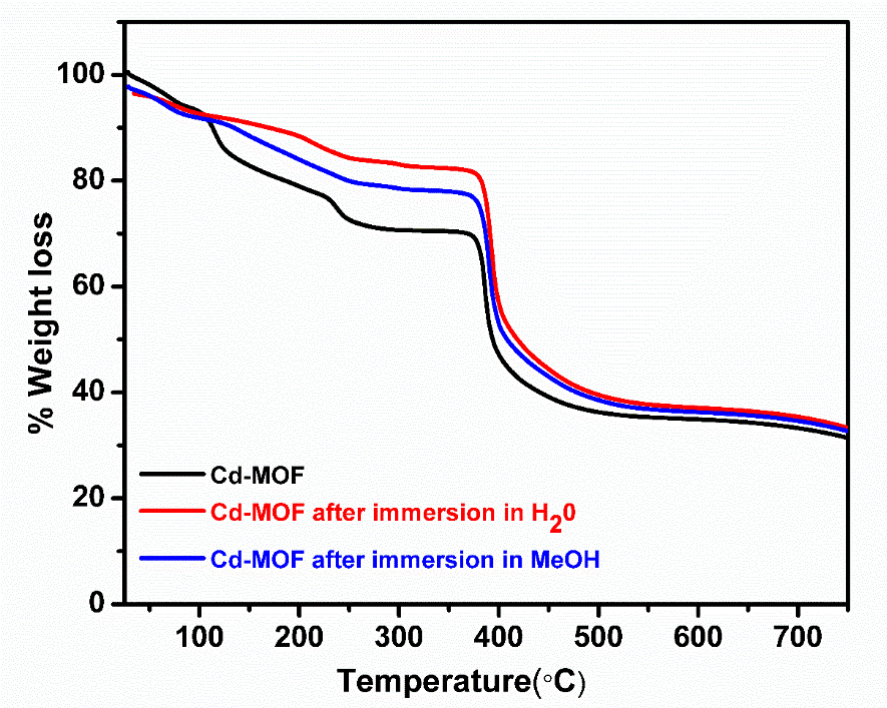

Fig. S15. TGA plot of **Cd-MOF** and the samples recovered after soaking in MeOH and H_2O for 24 h.

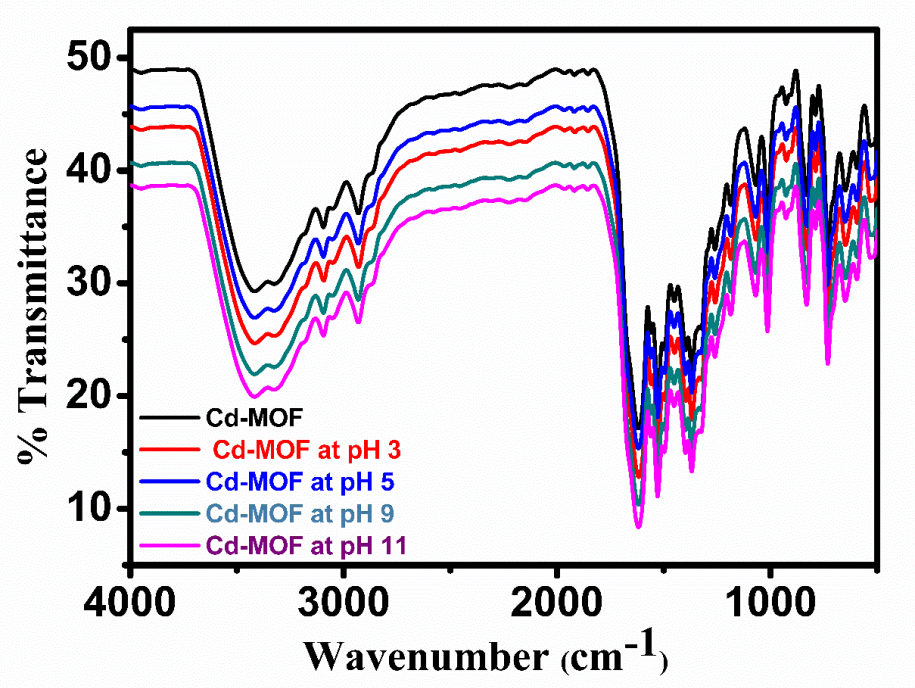

Fig. S16. FT-IR spectrum of **Cd-MOF** and the samples recovered after soaking in H_2O at different pH for 24 h**.**

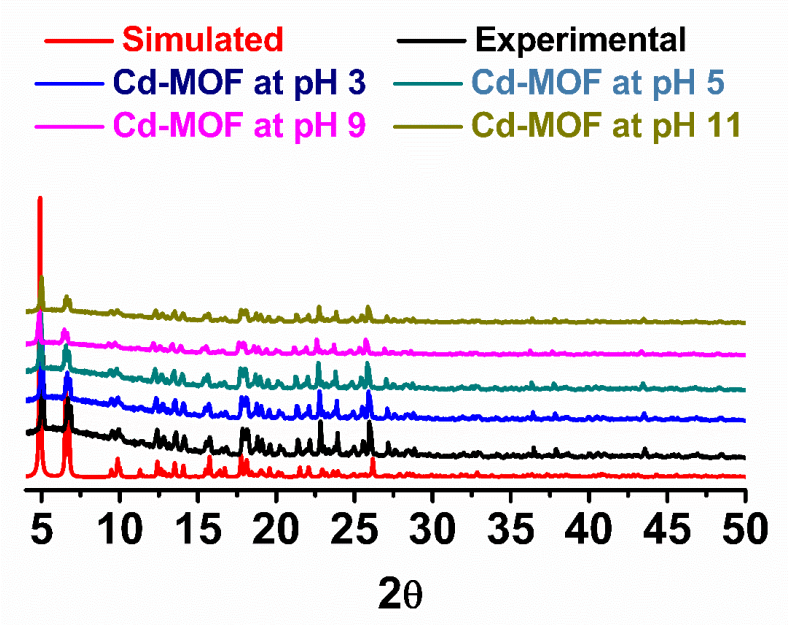

Fig. S17. PXRD patterns of **Cd-MOF** and the samples recovered after soaking in H_2O at different pH for 24 h.

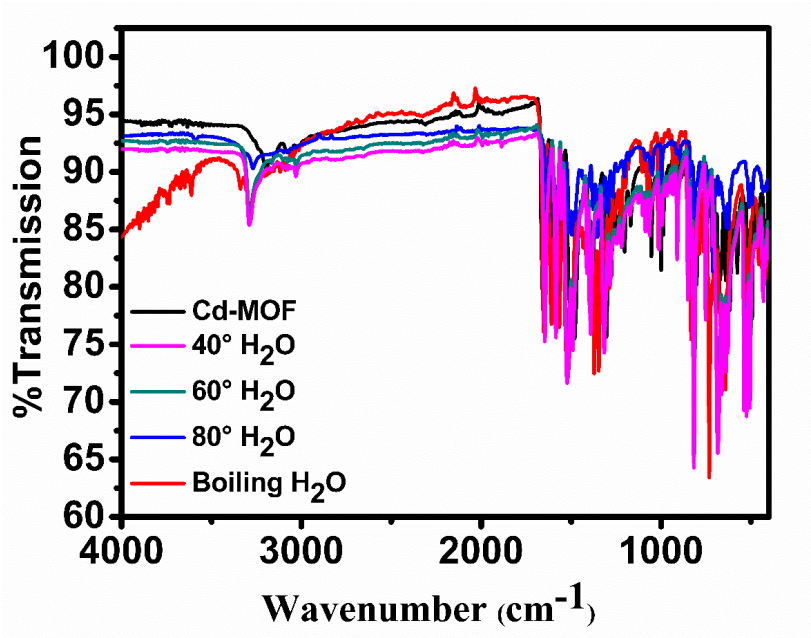

Fig. S18. FT-IR spectrum of **Cd-MOF** and the samples recovered after soaking in H_2O at different temperature for 24 h**.**

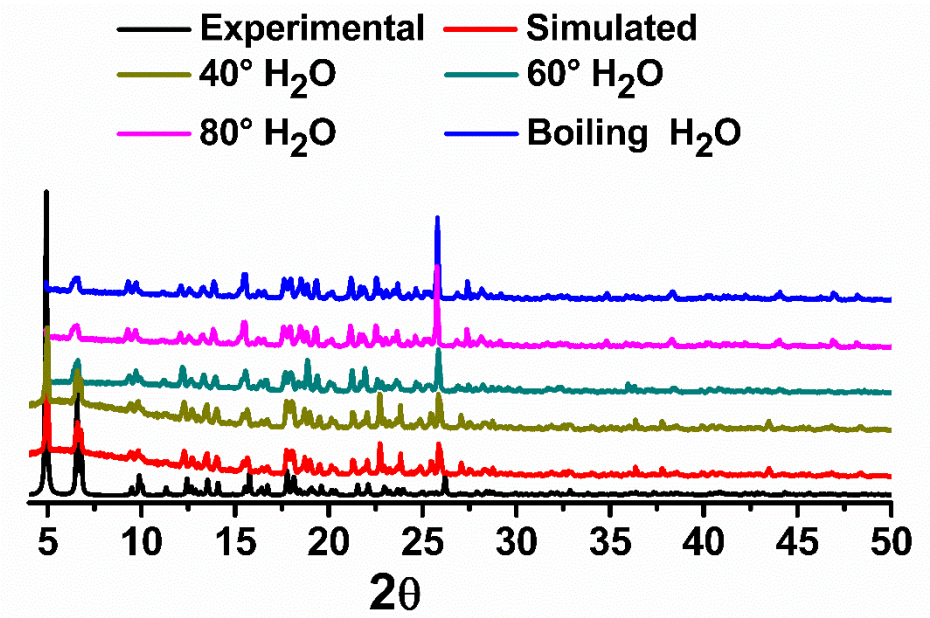

Fig. S19. PXRD patterns of **Cd-MOF** and the samples recovered after soaking in H_2O at different temperature for 24 h.

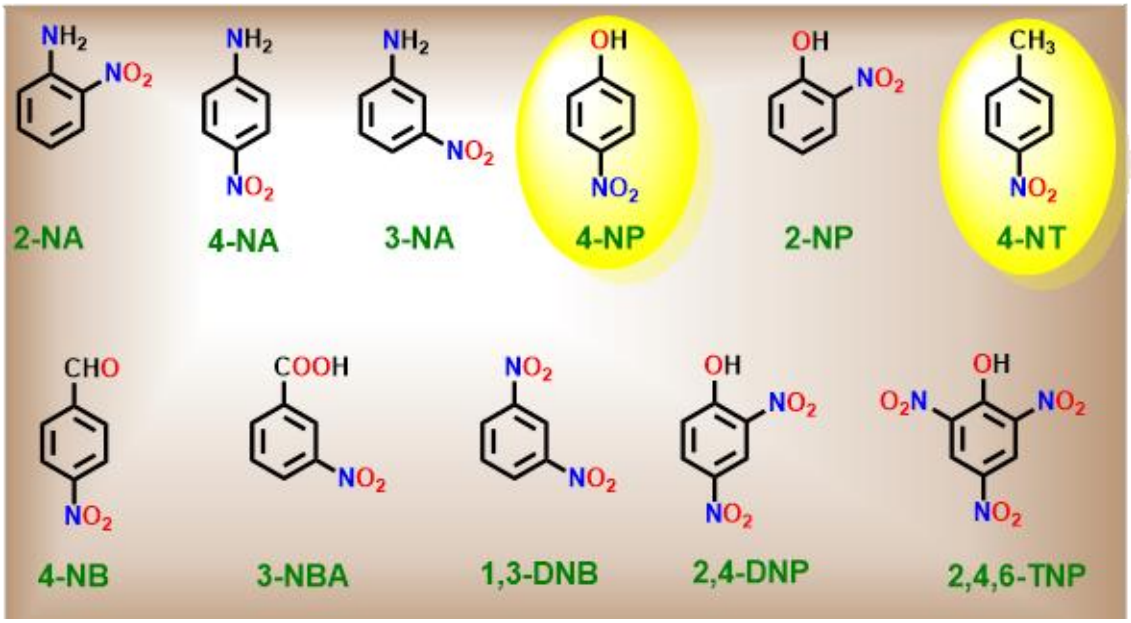

Chart S1. Chemical structures of nitroaromatics compounds used in the present sensing study.

Stern–Volmer constant (K_{SV}) and detection limit calculation:

Estimation of fluorescence titrations using the following Stern-Volmer equation.[S2]

$$I_0/I = 1 + K_{SV}[A] \qquad (1)$$

Where, I_0 = emission intensity without analyte

I = emission intensity with analyte

[A] = molar concentration of the analyte

K_{SV} = Stern-Volmer constant

The limit of detection (LOD) for the organic amine analytes were calculated using equation

$$\text{Detection limit: } 3\sigma/k \qquad (2)$$

Where, σ = standard deviation calculated from the blank measurements

k= slope of the titration plot of emission intensity

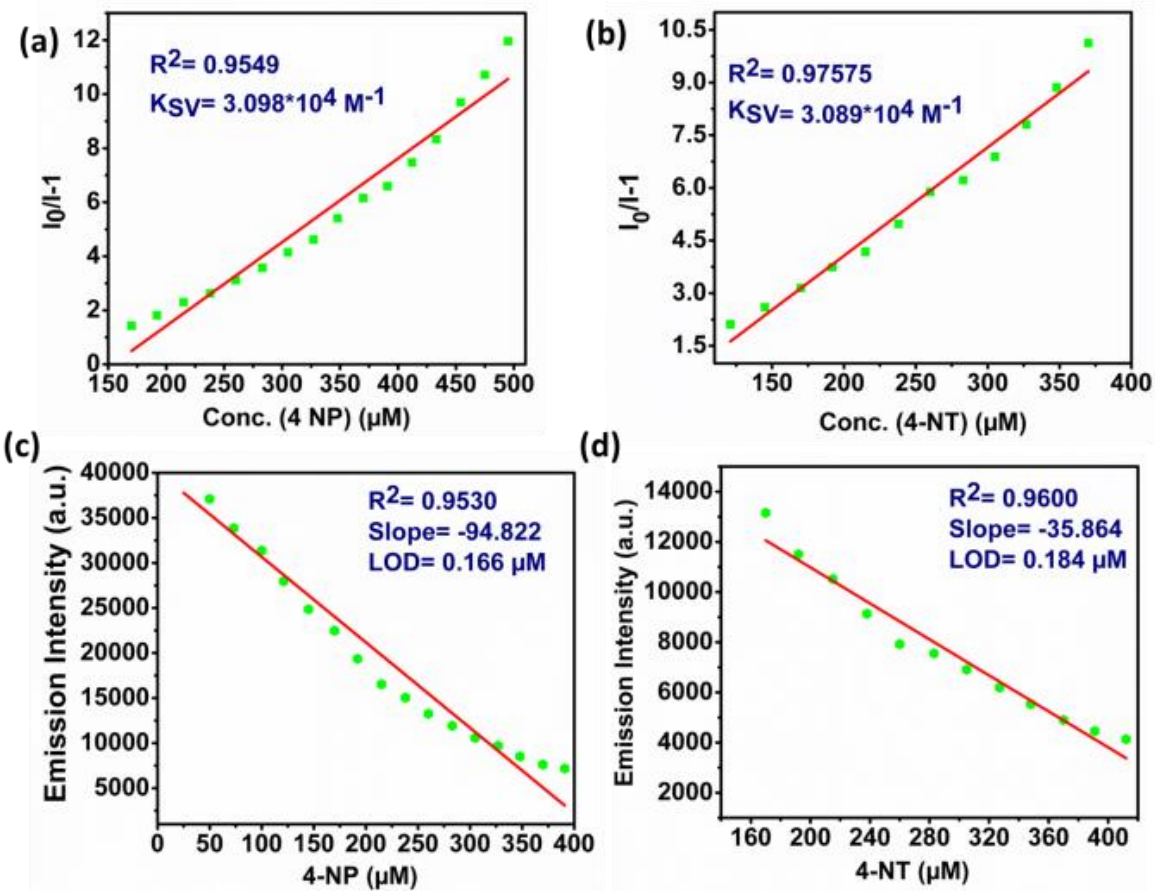

Fig. 20. (a, b) S−V plot for the recognition of 4-NP and 4-NT respectively. (c, d) Limit of detection calculation plots for the sensing of 4-NP and 4-NT by **Cd-MOF**.

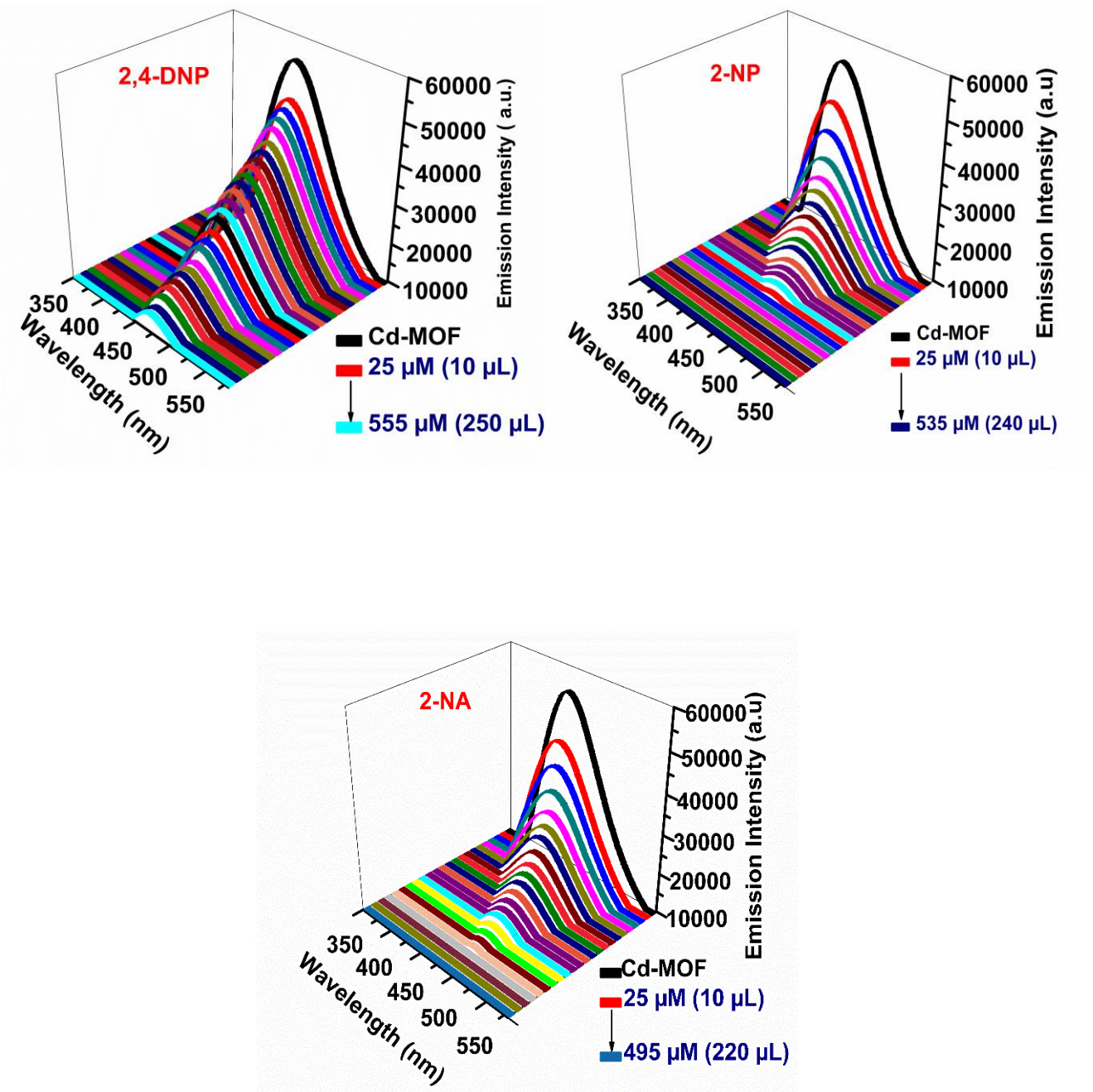

Fig. S21. The relative fluorescence intensity of **Cd-MOF** upon addition of solution of 2,4-DNP, 2-NP, 2-NA respectively**.**

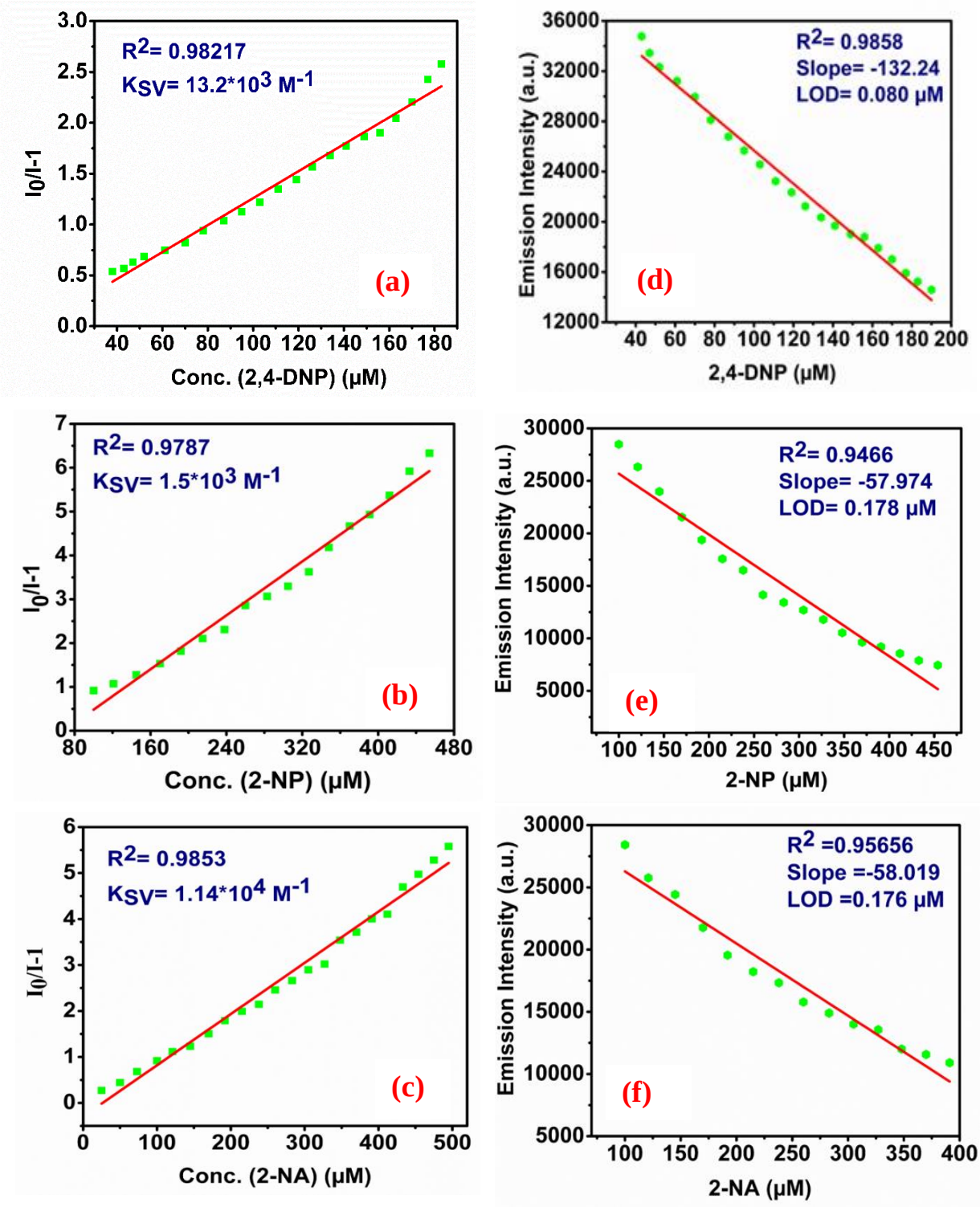

Fig. S22. (a-c) S−V plot for the recognition of 2,4-DNP, 2-NP and 2-NA respectively. (d-f) Limit of detection calculation plots for the sensing of 2,4-DNP, 2-NP and 2-NA analytes by **Cd-MOF** respectively.

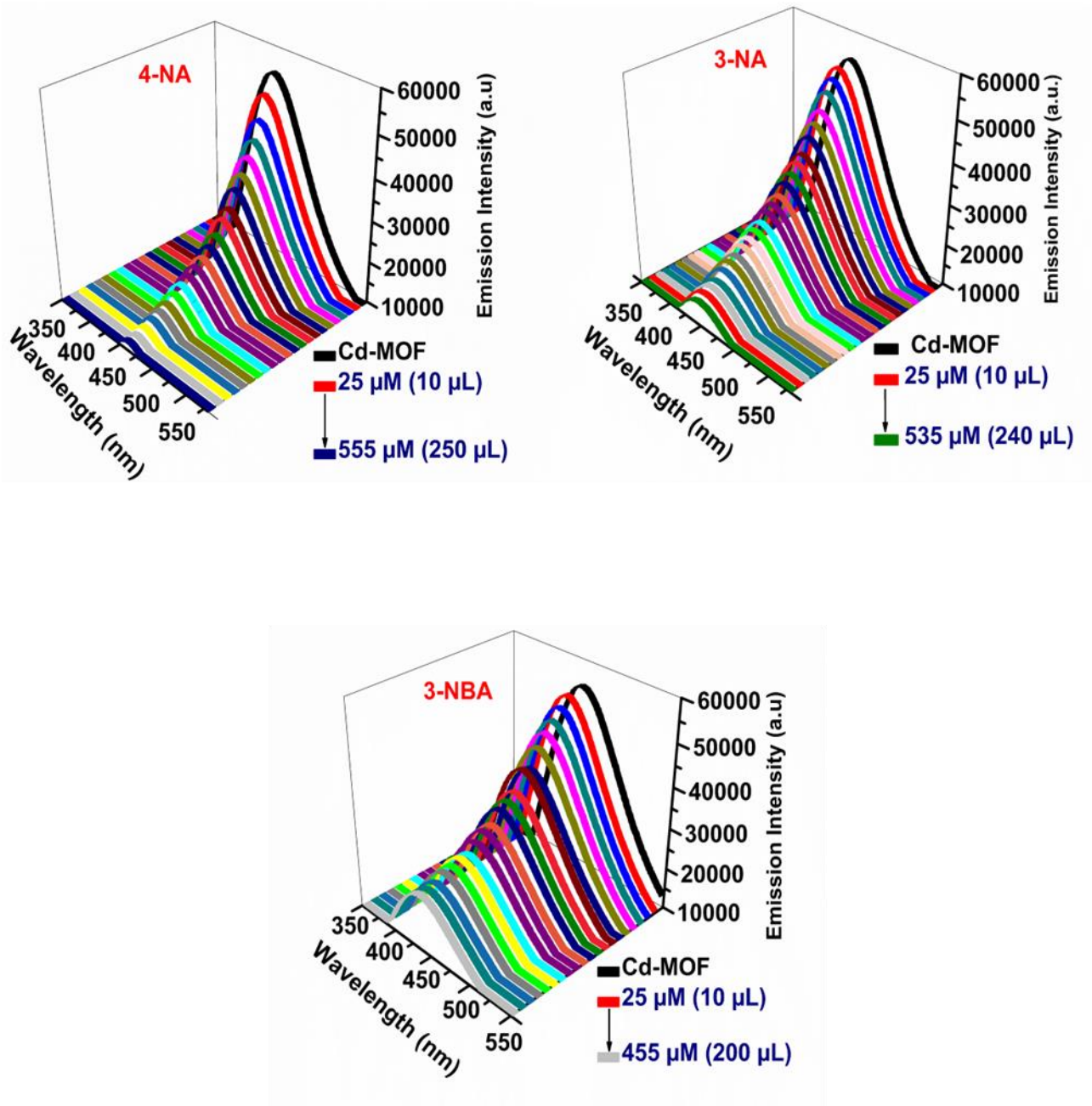

Fig. S23. The relative fluorescence intensity of **Cd-MOF** upon addition of solution of 4-NA, 3-NA, 3-NBA respectively.

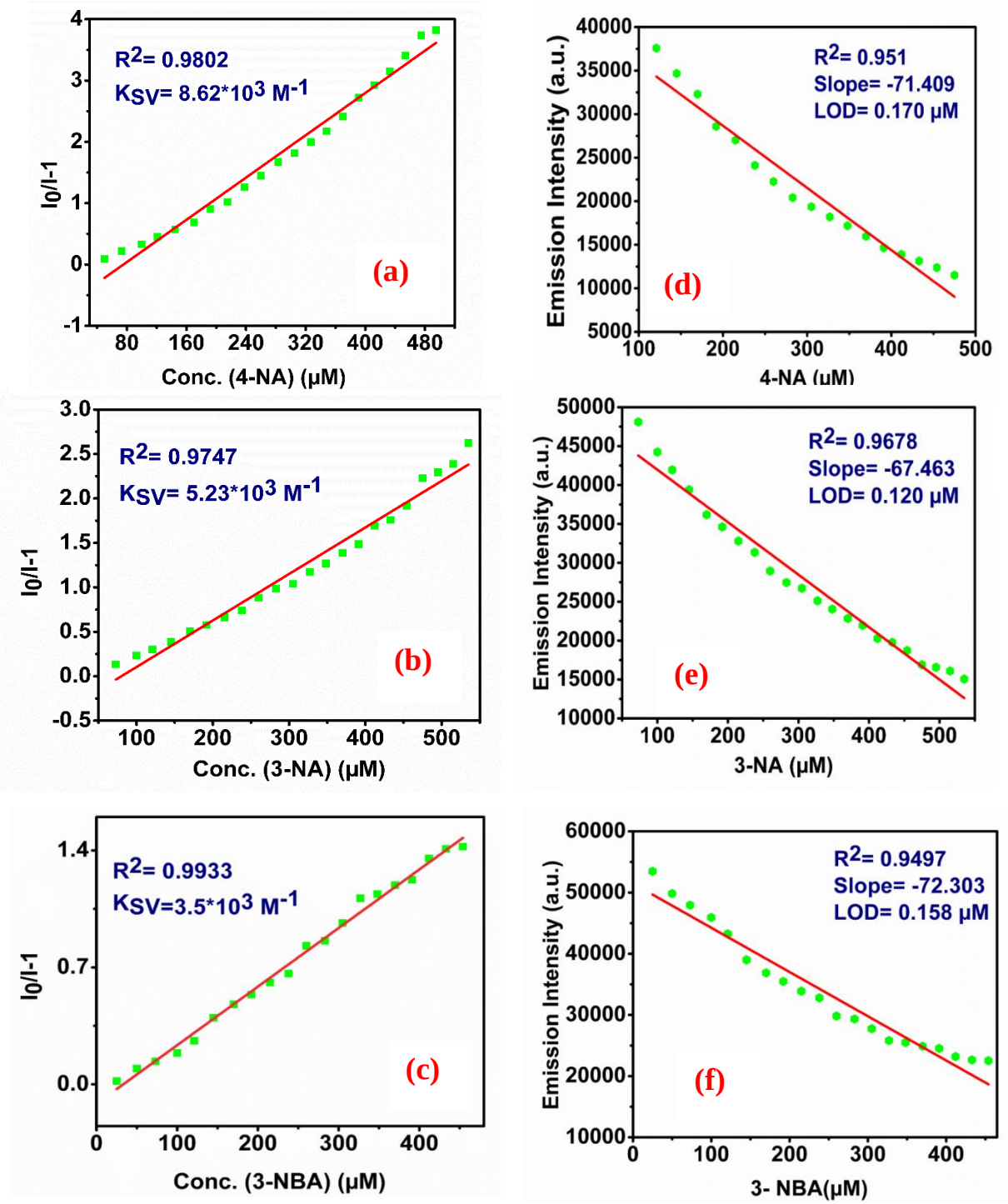

Fig. S24. (a-c) S–V plot for the recognition of 4-NA, 3-NA and 3-NBA respectively. (d-f) Limit of detection calculation plots for the sensing of 4-NA, 3-NA and 3-NBA analytes by **Cd-MOF** respectively.

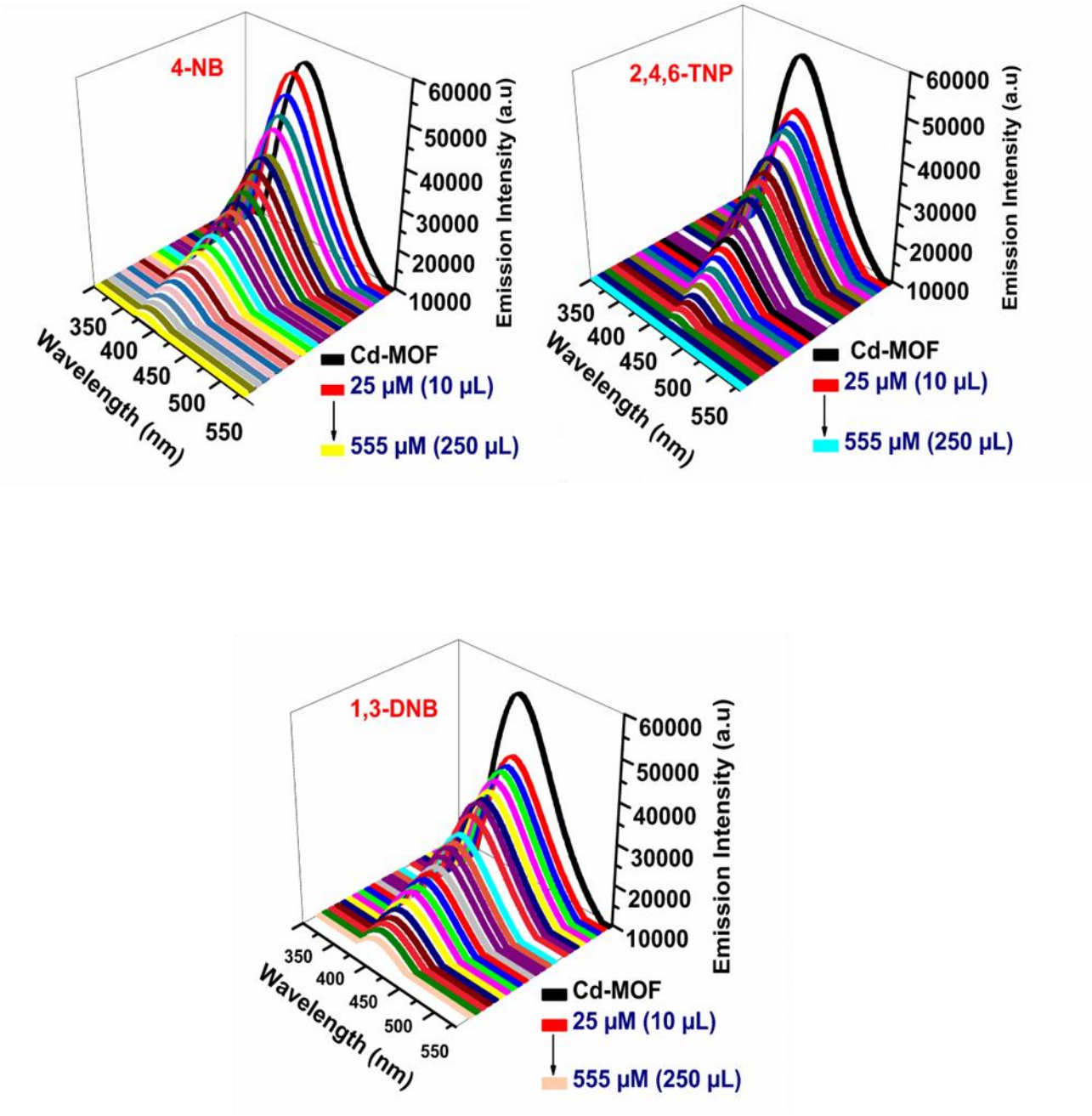

Fig. S25. The relative fluorescence intensity of **Cd-MOF** upon addition of solution of 4-NB, 2,4,6-TNP and 1, 3-DNB, respectively.

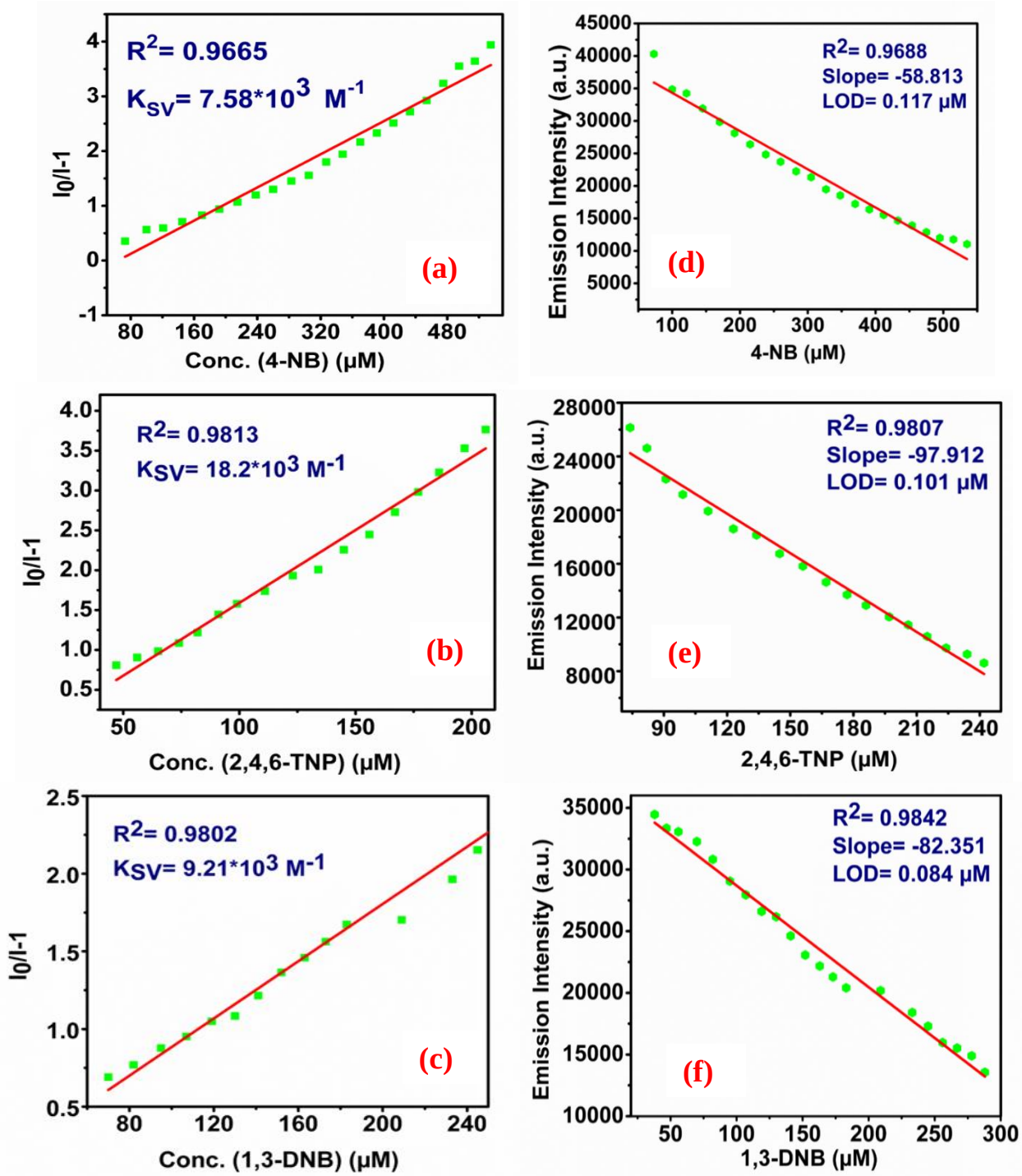

Fig. S26. (a-c) S−V plot for the recognition of 4-NB, 2,4,6-TNP and 1,3-DNB respectively. (d-f) Limit of detection calculation plots for the sensing of 4-NB, 2,4,6-TNP and 1,3-DNB analytes by **Cd-MOF** respectively.

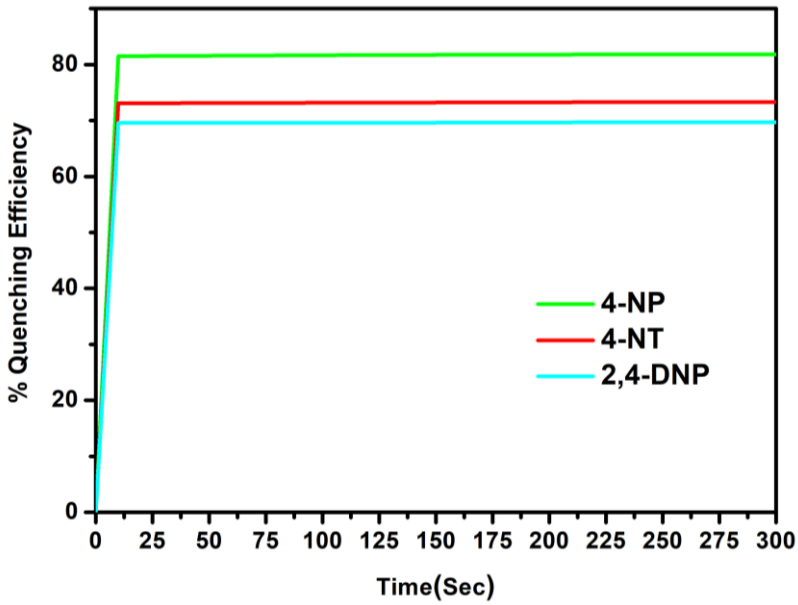

Fig. S27. Time dependent fluorescence response of **Cd-MOF** towards 4-NP, 4-NTand 2,4-DNP.

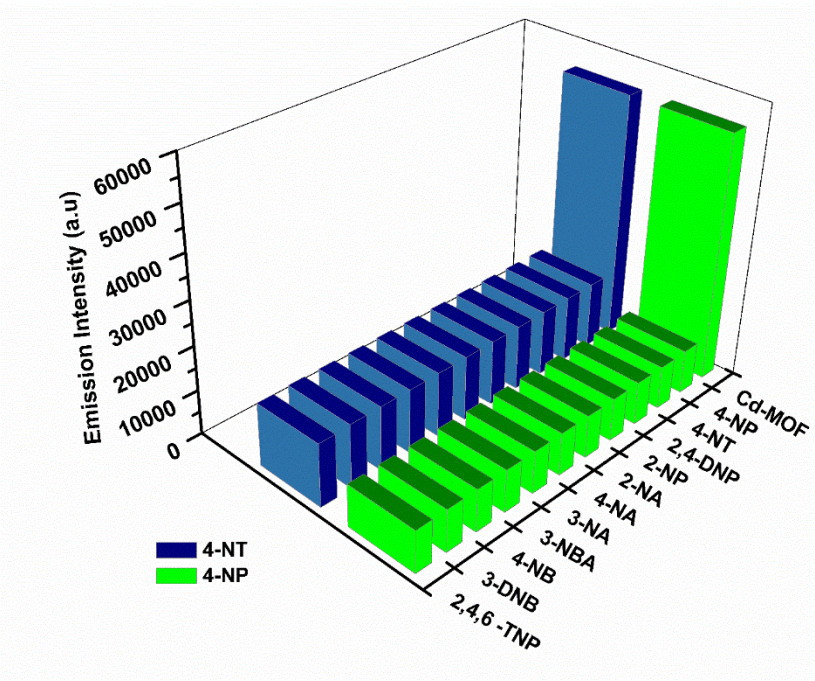

Fig. S28. Relative emission intensity of **Cd-MOF** upon addition of 50 µL of 4-NP and 4-NT (from 10 mM stock solution) in the presence of 50 µL of other nitroaromatics in CH_3OH.

Calculation of binding constant using Benesi-Hildebrand and fluorescence method:

Calculation of binding constant using Benesi-Hildebrand and fluorescence method: The value of binding constant of organic amines with **Cd-MOF** has been determined from the emission intensity data following the modified Benesi–Hildebrand equation.[S3]

$$1/\Delta I = 1/\Delta I_{max} + (1/K_b[C])(1/\Delta I_{max}) \qquad (3)$$

Here, $\Delta I = I - I_{min}$ and $\Delta I_{max} = I_{max} - I$, where I_{min}, I, and I_{max} are the emission intensities of sensor material measured in the absence of concern analytes, at an intermediate analyte's concentration, and at a concentration of complete saturation.

Whereas, K_b and [C] represent the binding constant and concentration of particular analytes, respectively. The K_b could be determined from the slope of a straight line of plot $1/(A-A_o)$ against 1/[Analyte].

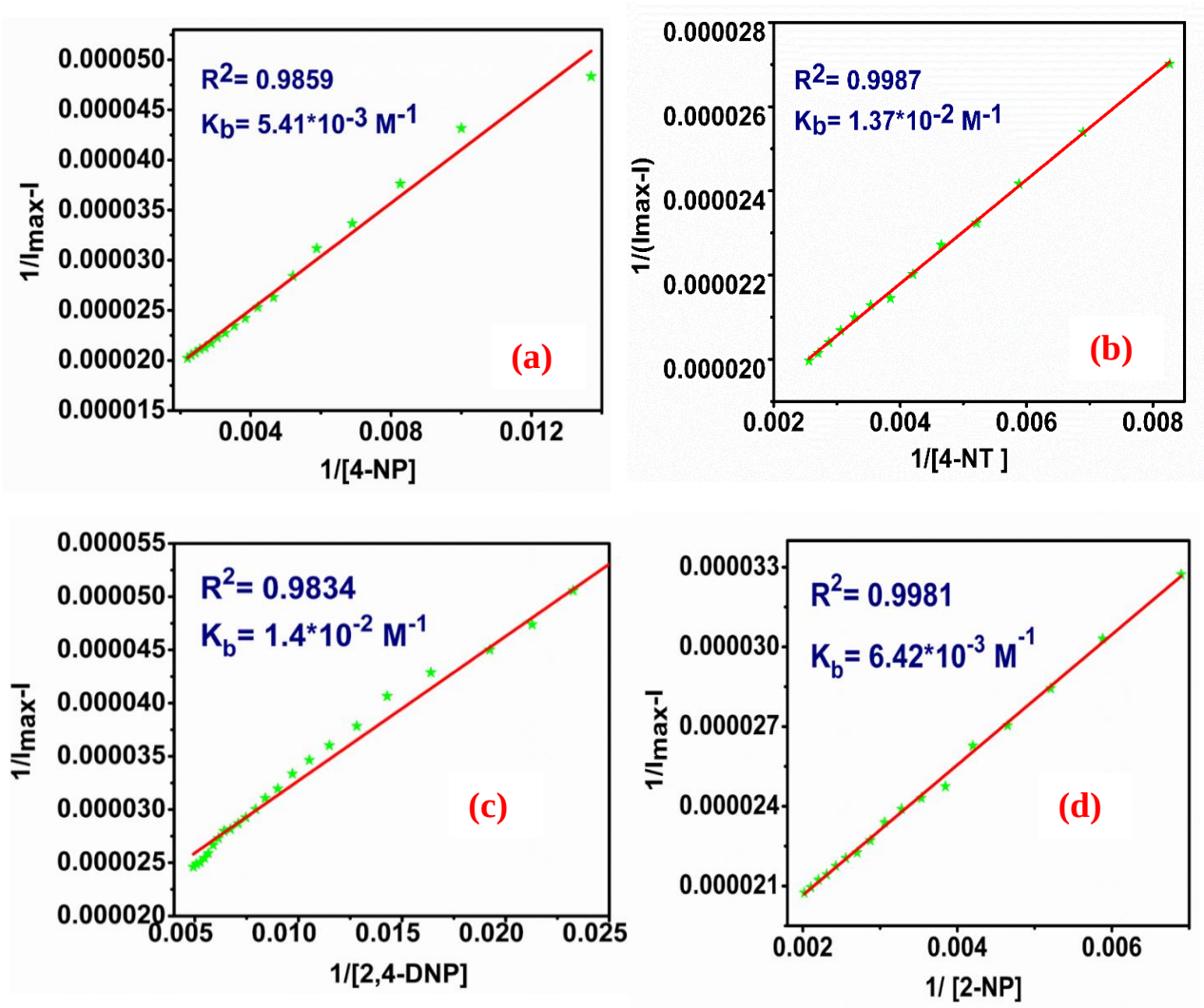

Fig. S29. (a-d) BH plot from the fluorescence titration data of receptor **Cd-MOF** (suspension) with 4-NP, 4-NT, 2,4-DNP and 2-NP respectively.

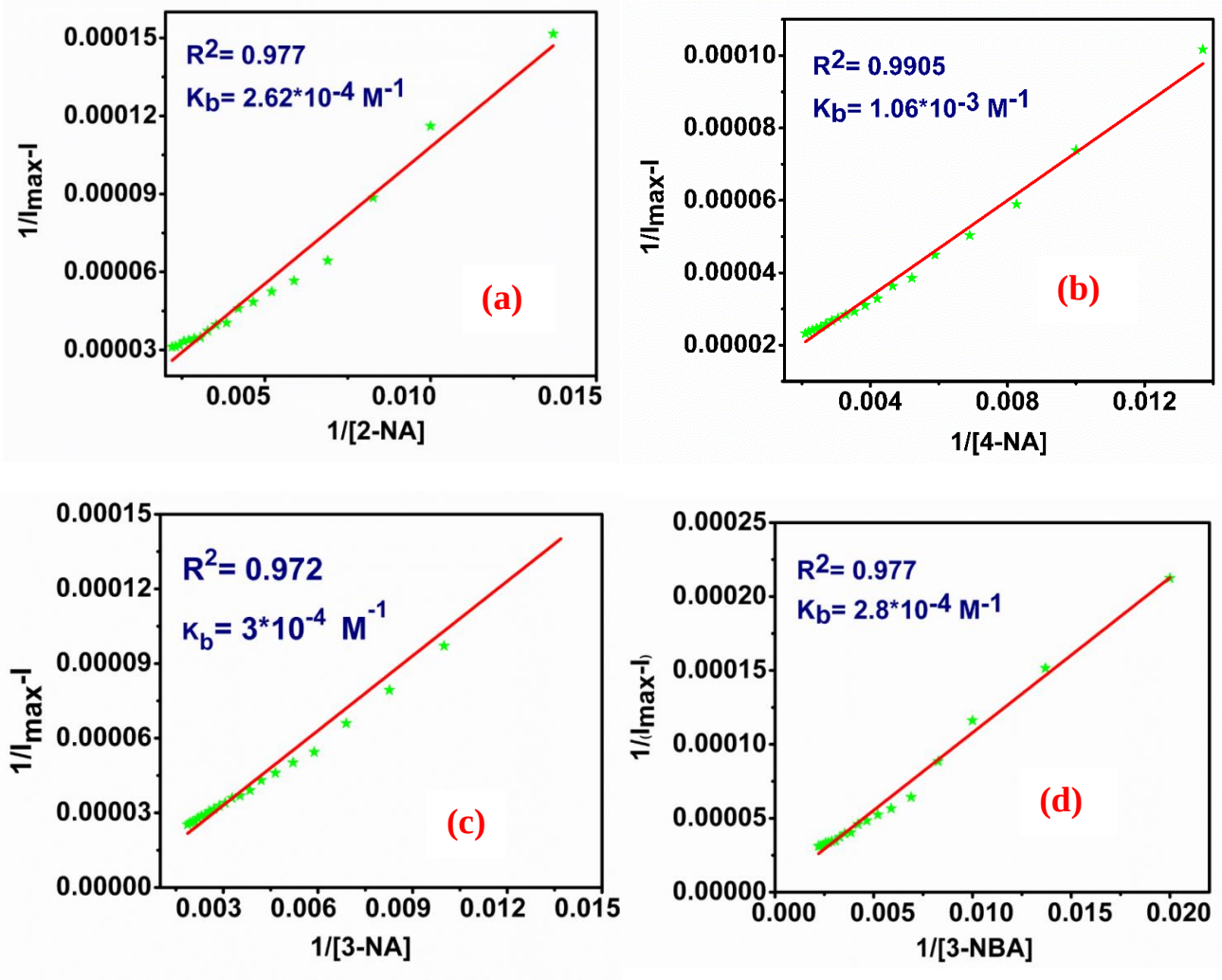

Fig. S30. (a-d) BH plot from the fluorescence titration data of receptor **Cd-MOF** (suspension) with 2-NA, 4-NA, 3-NA and 3-NBA respectively.

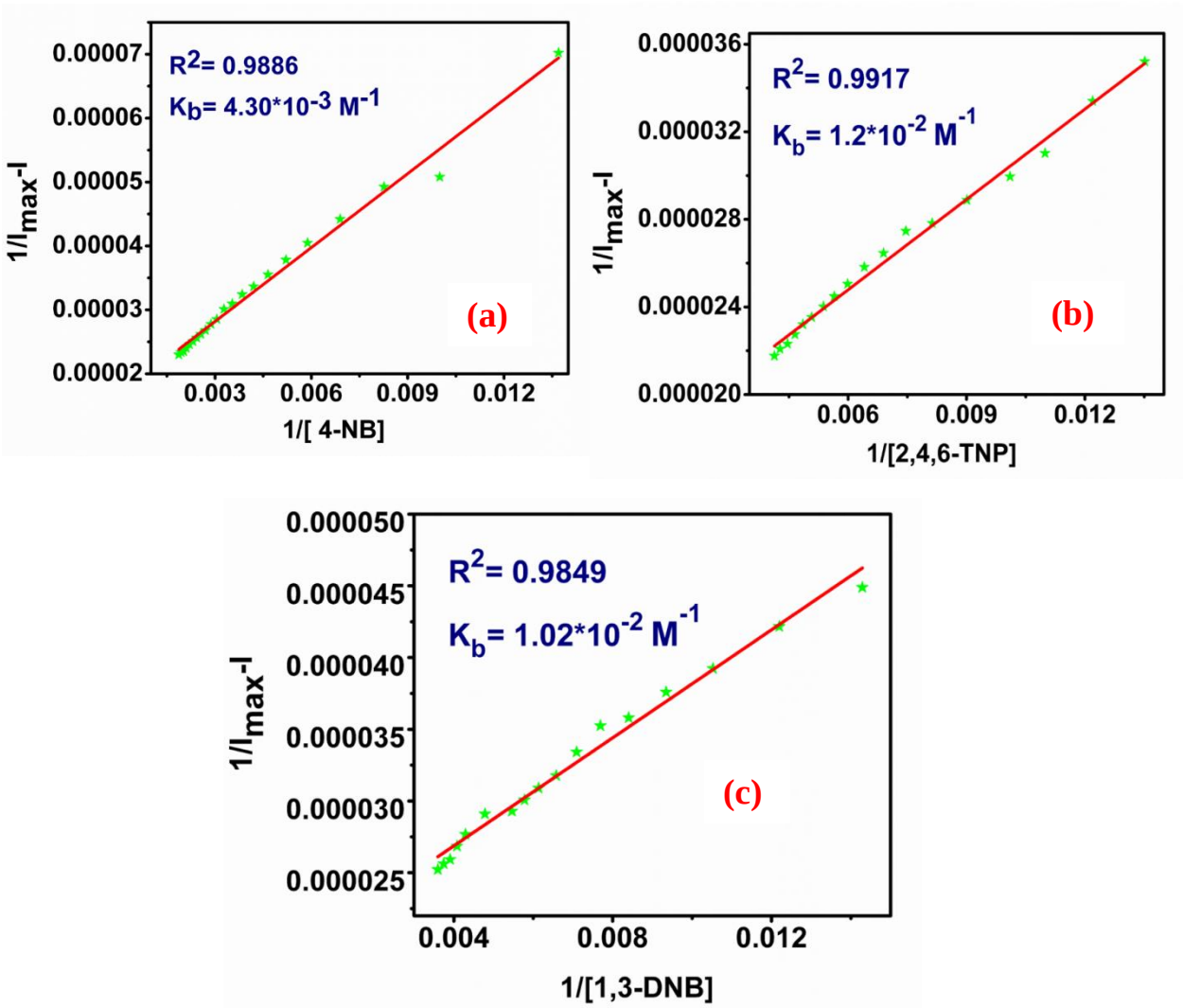

Fig. S31. (a-c) BH plot from the fluorescence titration data of receptor **Cd-MOF** (suspension) with 4-NB, 2,4,6-TNP and 1,3-DNB respectively.

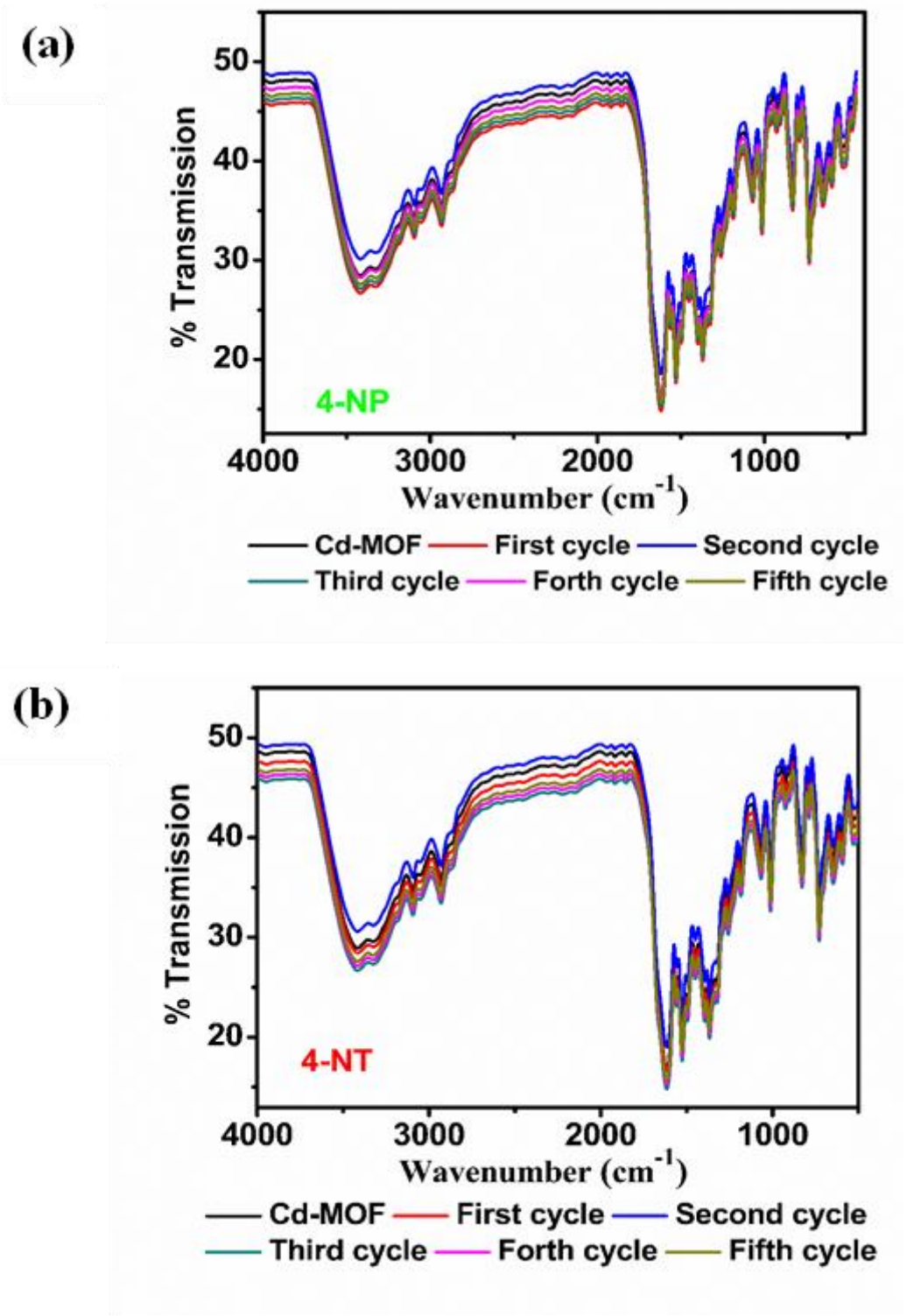

Fig. S32. (a-b) FT-IR patterns of original sample of **Cd-MOF** (black) and the recovered sample of **Cd-MOF** after each cycle of quenching with 4-NP and 4-NT respectively.

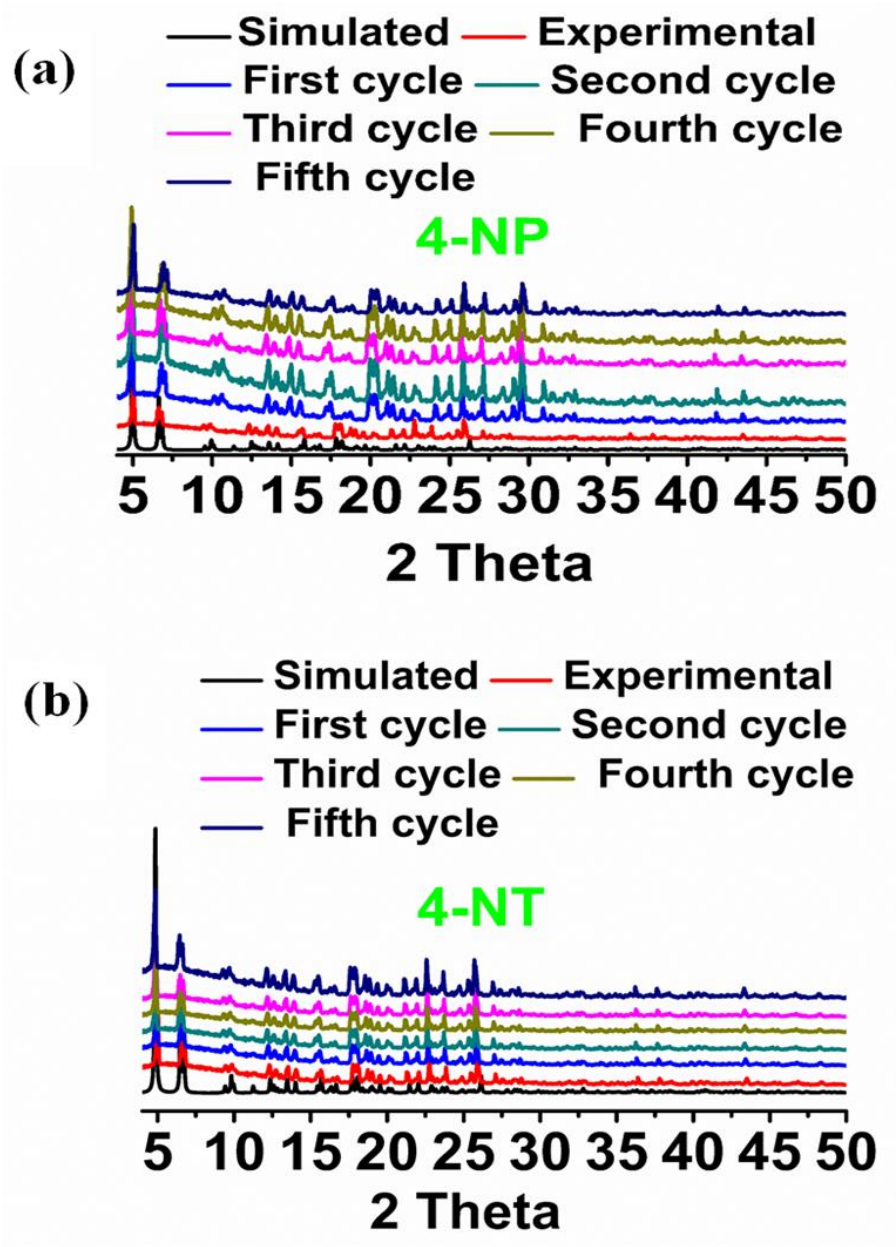

Fig. S33. (a-b) PXRD patterns of original sample of **Cd-MOF** (experimental, red trace; simulated, black) and the recovered sample of **Cd-MOF** after each cycle of quenching with 4-NP and 4-NT respectively.

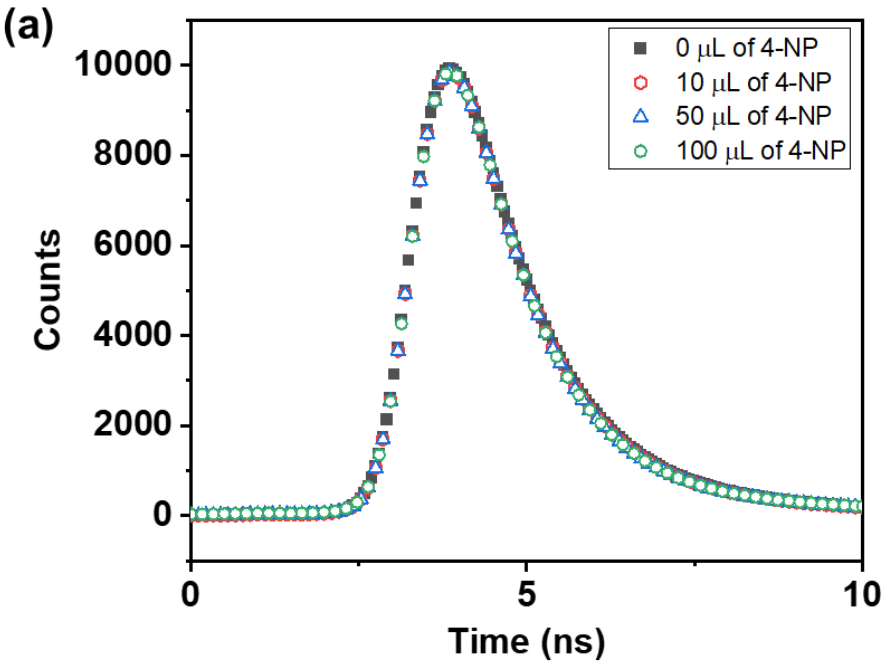

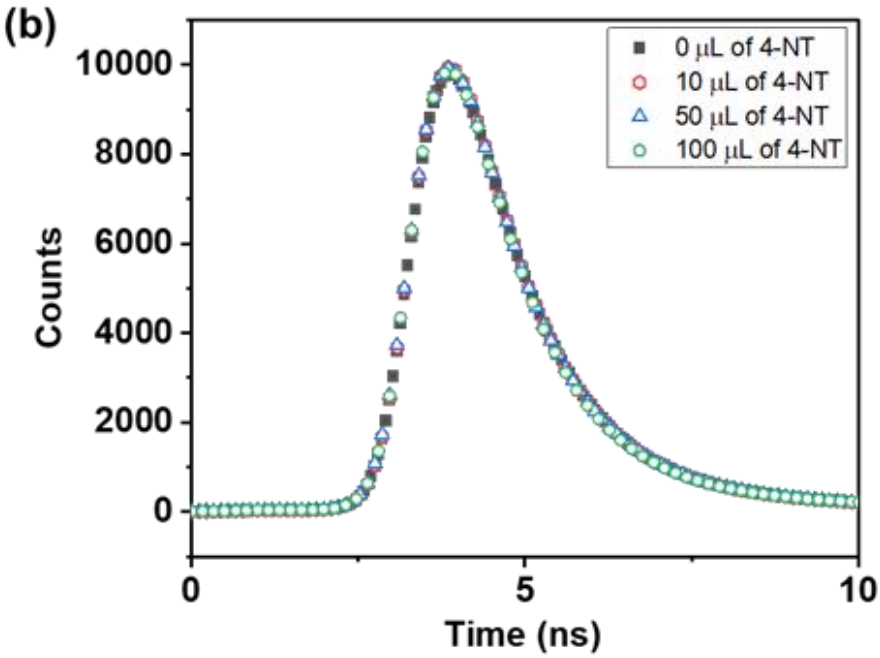

Fig. S34. (a-b) Lifetime decay curves of **Cd-MOF** before and after the addition of 4-NP and 4-NT, respectively.

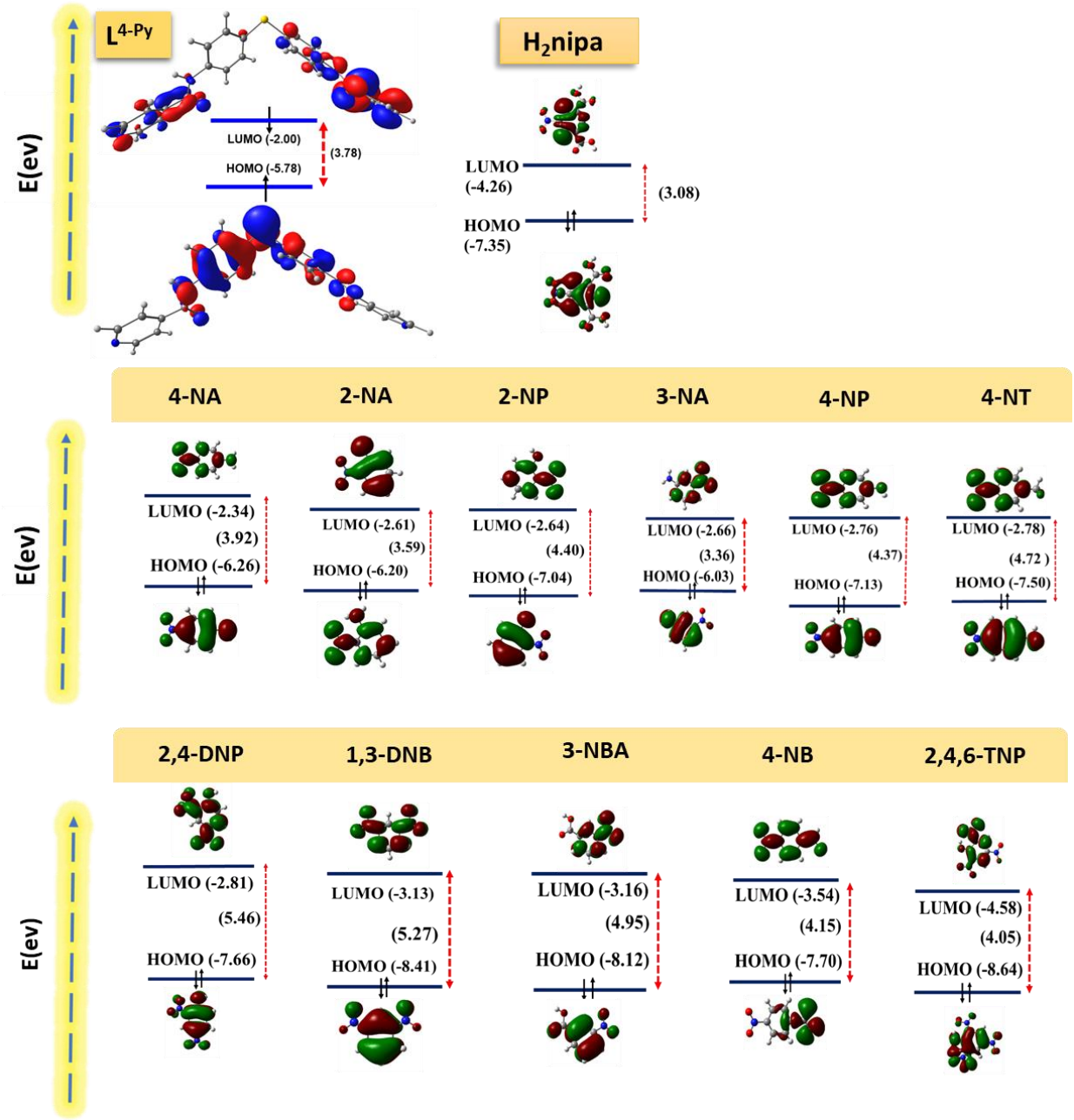

Fig. S35. Theoretically optimized HOMO and LUMO energies of **L$^{4\text{-py}}$**, H_2nipa and examined nitroaromatics using the B3LYP/6-31G protocol.

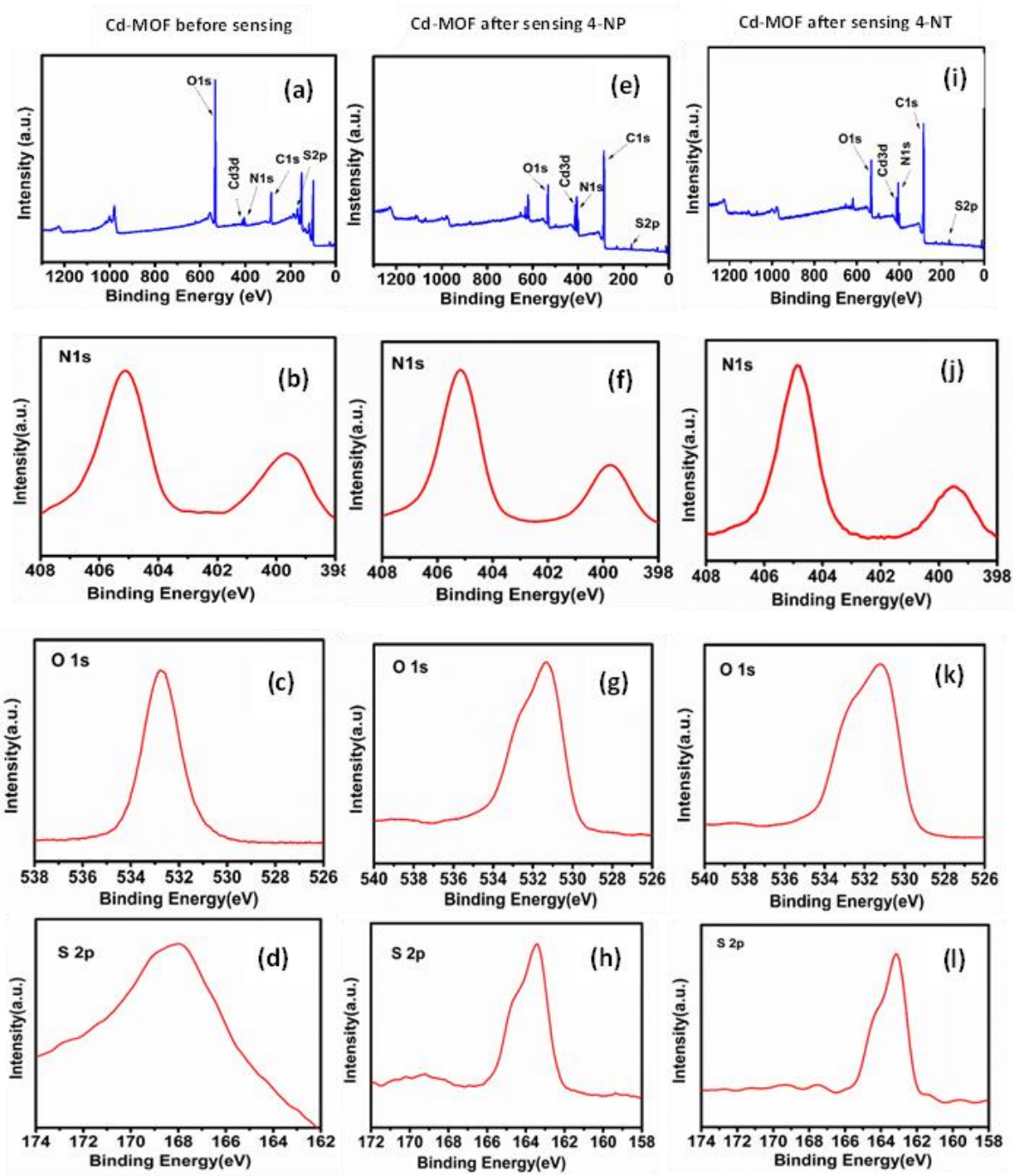

Fig. S36. (a) XPS spectrum of **Cd-MOF** before sensing. (b-d) XPS spectrum of **Cd-MOF** for N 1s, O 1s, S 2p before sensing. (e) XPS spectrum of **Cd-MOF** after sensing 4-NP. (f-h) XPS spectrum of **Cd-MOF** for N 1s, O 1s, S 2p after sensing 4-NP. (i) XPS spectrum of **Cd-MOF** after sensing 4-NT. (j-l) XPS spectrum of Cd-MOF for N 1s, O 1s, S 2p after sensing 4-NT.

Table S1. Crystal data and structure refinement for **$L^{4\text{-Py}}$** and **Cd-MOF**.

	$L^{4\text{-Py}}$	**Cd-MOF**
CCDC number	**2371129**	**2371128**
Empirical formula	$C_{24}H_{18}N_4O_2S$	$C_{40}H_{40}CdN_7O_{11}S$
Formula weight	426.48	939.25
Temperature [K]	293(2)	220(80)
Crystal system	triclinic	monoclinic
Space group (number)	$P\overline{1}$ (2)	$C2/c$ (15)
a [Å]	9.3689(3)	37.8579(8)
b [Å]	12.8121(3)	9.96330(10)
c [Å]	18.4744(3)	28.3070(6)
α [°]	98.161(2)	90
β [°]	90.769(2)	109.014(2)
γ [°]	111.088(2)	90
Volume [Å^3]	2043.11(9)	10094.5(3)
Z	4	8
ρ_{calc} [gcm^{-3}]	1.386	1.236
μ [mm^{-1}]	0.188	0.530
F(000)	888	3848
Crystal colour	Colourless	Yellow
Crystal shape	Block	block
Radiation	Mo K_α (λ=0.71073 Å)	Mo K_α (λ=0.71073 Å)
2θ range [°]	6.69 to 54.78 (0.77 Å)	6.25 to 54.91 (0.77 Å)
Index ranges	$-12 \le h \le 12$; $-15 \le k \le 16$; $-23 \le l \le 23$	$-47 \le h \le 47$; $-12 \le k \le 12$; $-36 \le l \le 36$
Reflections collected	19420	68409
Independent reflections	7699; R_{int} = 0.0375; R_{sigma} = 0.0502	10864; R_{int} = 0.0624; R_{sigma} = 0.0464
Completeness to θ = 26.000°	91.4 %	99.5 %
Data / Restraints / Parameters	7699/0/559	10864/495/434
Absorption correction T_{min}/T_{max} (method)	0.962/0.972 (multi-scan)	0.57767/1.00000 (multi-scan)
Goodness-of-fit on F^2	1.118	1.071
Final *R* indexes [$I \ge 2\sigma(I)$]	R_1 = 0.0519; wR_2 = 0.1276	R_1 = 0.0412; wR_2 = 0.1228
Final *R* indexes [all data]	R_1 = 0.0825; wR_2 = 0.1423	R_1 = 0.0546; wR_2 = 0.1367
Largest peak/hole [eÅ^{-3}]	0.29/−0.24	0.58/-0.53

Table S2. Selected bond length and angles for **Cd-MOF**.

Bond	Bond Length	Bond	Bond Angles
Cd1–O4$^{\#1}$	2.506(2)	O1–Cd1–O2	96.53(9)
Cd1–O2	2.496(2)	O1–Cd1–O5$^{\#1}$	90.57(9)
Cd1–O5$^{\#1}$	2.322(2)	O1–Cd1–N4$^{\#2}$	169.43(9)
Cd1–O1	2.318(3)	O1–Cd1–N1	85.65(9)
Cd1–O3	2.279(2)	O1–Cd1–C8$^{\#1}$	85.98(10)
Cd1–N4$^{\#2}$	2.364(3)	O3–Cd1–O4$^{\#1}$	131.19(7)
Cd1–N1	2.334(3)	O3–Cd1–O2	54.50(7)
Cd1–C8$^{\#1}$	2.744(3)	O3–Cd1–O5$^{\#1}$	77.02(8)
S1–C18	1.780(3)	O3–Cd1–O1	94.53(10)
S1–C21	1.780(4)	O3–Cd1–N4$^{\#2}$	95.91(10)
Bond	**Bond Angles**	O3–Cd1–N1	142.03(9)
O4$^{\#1}$–Cd1–C8$^{\#1}$	27.10(7)	O3–Cd1–C8$^{\#1}$	104.10(8)
O2–Cd1–O4$^{\#1}$	174.07(7)	N4$^{\#2}$–Cd1–O4$^{\#1}$	89.30(8)
O2–Cd1–C8$^{\#1}$	158.53(8)	N4$^{\#2}$–Cd1–O2	88.27(8)
O5$^{\#1}$–Cd1–O4$^{\#1}$	54.21(7)	N4$^{\#2}$–Cd1–C8$^{\#1}$	93.01(9)
O5$^{\#1}$–Cd1–O2	131.34(7)	N1–Cd1–O4$^{\#1}$	86.72(8)
O5$^{\#1}$–Cd1–N4$^{\#2}$	93.32(8)	N1–Cd1–O2	87.69(8)
O5$^{\#1}$–Cd1–N1	140.93(8)	N1–Cd1–N4$^{\#2}$	85.14(10)
O5$^{\#1}$–Cd1–C8$^{\#1}$	27.19(8)	N1–Cd1–C8$^{\#1}$	113.77(9)
O1–Cd1–O4$^{\#1}$	85.01(9)		

Symmetry transformations used to generate equivalent atoms: (#1) +X, -1+Y, +Z; (#2) 1.5-X, 0.5-Y, 1-Z; (#3) +X, 1+Y, +Z.

Table S3. Hydrogen bonding for ligand **$L^{4\text{-}Py}$**.

D–H···A [Å]	d(D–H) [Å]	d(H···A) [Å]	d(D···A) [Å]	<(DHA) [°]
N7–H7···O2$^{\#1}$	0.86	2.17	2.929(2)	147.6
N6–H6···N4$^{\#2}$	0.86	2.12	2.964(2)	165.9
C45–H45···O1$^{\#3}$	0.93	2.63	3.547(3)	169.4
C35–H35···N1$^{\#3}$	0.93	2.67	3.344(3)	129.5
C36–H36···O4	0.93	2.33	2.919(3)	121.3
C39–H39···O3	0.93	2.35	2.899(3)	117.7
N3–H3···N5$^{\#4}$	0.86	2.11	2.970(2)	173.9
N2–H2···O3	0.86	2.39	3.131(2)	144.7
C8–H8···S2$^{\#5}$	0.93	2.92	3.441(2)	117.0
C24–H24···O4$^{\#6}$	0.93	2.56	3.464(3)	164.0
C12–H12···O1	0.93	2.31	2.908(3)	121.4
C15–H15···O2	0.93	2.27	2.881(3)	123.1
C22–H22···S2$^{\#7}$	0.93	3.01	3.929(3)	168.9

Symmetry transformations used to generate equivalent atoms: #1: 1+X, +Y, +Z; #2: 1+X, +Y, 1+Z; #3: 1-X, 1-Y, 1-Z; #4: +X, +Y, -1+Z; #5: -1+X, +Y, +Z; #6: 1-X, 1-Y, -Z; #7: -X, -Y, -Z.

Table S4. Hydrogen bonding for **Cd-MOF**.

D–H···A [Å]	d(D–H) [Å]	d(H···A) [Å]	d(D···A) [Å]	<(DHA) [°]
O1–H1A···O8$^{\#1}$	0.90	2.05	2.816(4)	142.5
C20–H20···O8	0.94	2.23	2.833(4)	121.4

Symmetry transformations used to generate equivalent atoms: (#1): 1-X, -Y, 1-Z;

Table S5. Fluorescence quantum yields of the **$L^{4\text{-}Py}$**, H_2nipa and **Cd-MOF**.

S.No.	Compound	Wavelength λ_{ex} (λ_{em}) [nm]	Fluorescence Quantum Yield (ϕ_F)	Stokes Shift
1	**$L^{4\text{-}py}$**	300(435)	0.25	135
2	H_2nipa	285(436)	0.18	151
3	**Cd-MOF**	290 (444)	0.40	154

Quantum yield (Φ) is defined as the ratio of the number of photons emitted to the number of photons absorbed. For the measurements of quantum yield of **$L^{4\text{-}py}$**, co-ligand H_2nipa, and **Cd-MOF**, the standards used were 2-Amino-pyridine in H_2SO_4, naphthalene in cyclohexane, and 9,10-Diphenylanthracene in cyclohexane, respectively. It is important to mention that **Cd-MOF** exhibits the highest 40.30% (Φ_F = 0.40) of fluorescence quantum yields when excited at 290 nm. Whereas under identical conditions, ligand **$L^{4\text{-}py}$** and co-ligand H_2nipa show quantum yields of 25.30% (Φ_F = 0.25) and 18.40% (Φ_F = 0.18), when excited at 300 and 285 nm, respectively. [S4]

Table S6. Stern−Volmer (SV) quenching constant and detection limits of all examined analytes.

Sr. No.	Nitroanalytes	LOD (μM)	K_{sv} (M^{-1})	K_b (M^{-1})
1.	2-NA	0.176	1.14×10^4	2.62×10^{-4}
2.	3-NA	0.120	5.23×10^3	3.00×10^{-4}
3.	4-NA	0.170	8.62×10^3	1.06×10^{-3}
4.	2-NP	0.178	1.5×10^3	6.42×10^{-3}
5.	4-NP	0.166	3.09×10^4	5.41×10^{-3}
6.	4-NT	0.184	3.09×10^4	1.37×10^{-2}
7.	4-NB	0.117	7.58×10^3	4.30×10^{-3}
8.	3-NBA	0.158	3.5×10^3	2.8×10^{-4}
9.	1,3-DNB	0.084	9.21×10^3	1.02×10^{-2}
10.	2,4-DNP	0.080	13.2×10^3	1.4×10^{-2}
11.	2,4,6-TNP	0.101	18.2×10^3	1.2×10^{-2}

.

Table S7. A comparative list of various fluorescent MOFs including **Cd-MOF** that have been used for sensing of various nitroaromatics.

CPs / MOFs	Analytes	Quenching constant (K_{sv}, M^{-1})	Limit of detection (μM)	Solvent	Ref.
$[Cd(\mathbf{L^{4\text{-}Py}})(nipa)(H_2O)]_n$ (**Cd-MOF**)	4-NP	3.098×10^4	0.166	Methanol	In this work
$[Cd_3(BPPA)_3(aba)_3]_n$	4-NP	6.74×10^4	34.48 ppb	DMF	S5
$[Cd_2(HL^1)(btc)(H_2O)_2].3H_2O$	4-NP	2.69×10^4	0.575	DMF	S6
Zn(DMA)(TBA)	4-NP	4.39×10^4	1.43	Ethanol	S7
$[Zn(L^2)(H_2O)].H_2O$	4-NP	1.25×10^4	3.74	Water	S8
$\{[Zn_3(mtrb)_3(btc)_2].3H_2O\}_n$	4-NP	1.276×10^4	2.56	Methanol	S9
$[Cd(ppvppa)(1,4\text{-}NDC)]_n$	2,4-DNP/ 4-NP	118 / 15	70 ppm / 120 ppm	Water	S10
$\{[Zn_2(L^3)(DMF)_3]\cdot 2DMF\cdot 2H_2O\}$	2,4-DNP/ 4-NP	2.40×10^4, 1.52×10^4	0.77 ppm / 1.03 ppm	DMF	S11
$(Zn_2(NDC)_2(bpy)\cdot Gx)$ (G = Guest molecules)	2,4-DNP/ 4-NP	1.5×10^{-4}/ 1.06×10^{-4}	0.284/ 0.347	Ethanol	S12
$[Cd(AA)(bpa)(OH_2)]_n$	4-NP	5.07×10^5	--	Water	S13
$[Zn_2(TCPE)(tta)_2]\cdot 2DMF\cdot 4H_2O\cdot 2Me_2NH_2^+$	4-NP	1621.97	0.68	DMF	S14
$[Cd_3(H_2O)_3(L^4)(tib)_2].5DMA.4H_2O$	4-NP	1.557×10^4	74	DMF	S15
$\{[(CH_3)_2NH_2]_2[Cd_3(TCPPDA)_2]\cdot 5DMF\cdot 8H_2O\}_n$	4-NP	3.25×10^5	7.5	DMF	S16
$\{(Me_2NH_2)_{10}[Zn_6L_4(\mu_3O)_2Zn_3]\cdot Gx\}_n$ (G = Guest molecules) (FJI-C8)	2,4-DNP	5.11×10^4	2.86	DMF	S17
$[Zn_4(Hbpvp)_2)BTC)_3(HCOO)H_2O)_2]\cdot 4H_2O$	2,4-DNP	--	1.0	Water	S18
$\{[Zn(L^5)]\cdot 4H_2O\cdot 2CH_3CN\}_n$	2,4-DNP/ 4-NP	3.07×10^4/ 8.21×10^4	8.49/ 4.49 mM	DMF	S19
$\{(NH_2(CH_3)_2)[Zn_4(ddn)_2(COO)(H_2O)_4]\cdot solvent\}_n$	2,4-DNP	8.93×10^3	1.12 ppm	DMF	S20

Abbreviation: $L^{4\text{-}Py}$ = *N,N'*-(thiobis(4,1-phenylene))diisonicotinamide; H_2nipa = 5-nitroisophthalic acid; BPPA = bis(4-(pyridine-4-yl)phenyl)amine), H_2aba = 4,4'-azanediyldibenzoic acid, H_2L^1 = 1-(1H-imidazol-4-yl)-4-(4H-tetrazol-5-yl)benzene), H_3btc = 1,3,5-benzenetricarboxylic acid, H_2TBA = 4-(1H-tetrazol-5-yl)-benzoic acid), DMA = Dimethylacetamide, H_2L^2 = 5-(2- methylpyridin-4-yl)isophthalic acid, mtrb = 1,3-bis(1,2,4- triazole-4-ylmethyl)benzene, ppvppa = N-(pyridin-2-yl)-N-(4-(2-(pyridin-4-yl)vinyl)phenyl)pyridin-2-amine, 1,4-H_2NDC = 1,4-naphthalenedicarboxylic acid, H_4L^3 = terphenyl-3,3'',5,5''-tetracarboxylic acid, NDC = 2,6- naphthalene dicarboxylic acid, bpy = 4,4' bipyridine, G = guest solvent molecules, AA = adipic acid, bpa = 1,2-bis(4- pyridyl)ethane), H_4TCPE = 1,1,2,2-tetra(4-carboxylphenyl)ethylene, 1H-tta = 1H-tetrazole, H_6L^4 = 5,5',5''-((benzene-1,3,5-tricarbonyl)tris(azanediyl))triisophthalic acid, tib = 1,3,5-tri(1H-imidazol-1-yl)benzene, H_4TCPPDA = N,N,N',N'-Tetrakis(4-carboxyphenyl)-1,4-phenylenediamine), FJI-C8 (*FJI stands for Fujian Institute of Research on the Structure of Matter, C stands for Cao's group, 8 stands for the number of newly synthesized crystals in his group*), bpvp = 3,5-

bis-(2-(pyridin-4-yl)vinyl)pyridine, H_2L^5 = 5-(3,5-Di-pyr-idin-4-yl-[1,2,4]triazol-1-ylmethyl)-isophthalic acid, H_4ddn=3,5-di(3,5-dicarboxylphenyl)nitrobenzene.

Table S8. Integral Orbital Overlap J(λ) values of nitro-analytes.

S.No.	Nitro analytes	J(λ)(M^{-1} cm^{-1} nm^4)
1	4-NP	3.3×10^8
2	4-NT	4.8×10^7
3	2,4-DNP	4.5×10^7
4	2-NP	3.5×10^7
5	2-NA	5.9×10^7
6	4-NA	2.5×10^7
7	3-NA	1.6×10^7
8	3-NBA	4.2×10^6
9	4-NB	3.7×10^6
10	2,4,6-TNP	1.9×10^6
11	1,3-DNB	1.8×10^6

Calculation of extent of overlapping.

The extent of overlapping of emission spectra of **Cd-MOF** with absorbance spectra of all nitroanalytes compounds has been calculated using formula (1) given below.[S21]

$$J(\lambda) = \int_0^{\infty} F_D(\lambda)\, \varepsilon_A(\lambda)\, \lambda^4\, d\lambda \quad \text{.....(1)}$$

Where F(λ) is the corrected fluorescence intensity of the donor (here **Cd-MOF**) in the range of λ to λ+Δλ with total intensity normalized to unity, ε_A is the molar extinction coefficient of the acceptor (here nitroanalytes) at λ in mol^{-1} cm^{-1}.

References.

S1. B.-C. Tzeng, T.-Y. Chang and H.-S. Sheu, *Chem. Eur. J.,* 2010, **16**, 9990-9993.

S2. A. Ganguly, B.K. Paul, S. Ghosh, S. Kar and N. Guchhait, *Analyst*, 2013, **138**, 6532-6541.

S3. S. Pandey, P. Kumar and R. Gupta, *Dalton Trans*., 2018, **47**, 14686-14695.

S4. A. M. Brouwer, Standards for photoluminescence quantum yield measurements in solution. *Pure Appl. Chem*., 2011, **83**, 2213-2228.

S5. Z. J. Wang, L. Qin, J-Xi. Chen and H.-G. Zheng, *Inorg. Chem.*, 2016, **55**, 10999–11005.

S6. X.-Z. Guo, S.-S. Chen, W.-D. Li, S.-S. Han, F. Deng, R. Qiao and Y. Zhao, *ACS Omega,* 2019, **4**, 11540-11553.

S7. X. Zhang, X. Luo, N. Zhang, J. Wu and Y.-Q. Huang, *Inorg. Chem. Front*., 2017, **4**, 1888-1894.

S8. X.-Y. Guo, F. Zhao, J.-J. Liu, Z.-L. Liu and Y.-Q. Wang, *J. Mater. Chem*. A, 2017, **5**, 20035.

S9. Y.-Q. Zhang, V. A. Blatov, T.-R. Zheng, C.-H. Yang, L.-L. Qian, K. Li, B.-L. Li and B. Wu, *Dalton Trans*., 2018, **47**, 6189-6198.

S10. M.-M. Chen, X. Zhou, H.-X. Li, X.-X. Yang and J.-P. Lang, *Cryst. Growth Des*., 2015, **15**, 2753–2760.

S11. J.-C. Jin, J. Wu, Y.-X. He, B.-H. Li, J.-Q. Liu, R. Prasad, A. Kumar and S. R. Batten, *CrystEngComm*, 2017, **19**, 6464-6472.

S12. N. Kajal, and S. Gautam, *Chem. Eng. J. Adv*., 2022, **11**, 100348.

S13. N. Goel and N. Kumar, *Inorganica Chim. Acta*., 2020, **53**, 119352.

S14. X. Zhang, G. Ren, M. Li, W. Yang and Q. Pan, *Cryst. Growth Des*., 2019, **19**, 6308-6314.

S15. X.-Yu. Sun, X.-D. Zhangb, Z.-H. Xub, Y. Zhaob, Z.-L. Wanga and W.-Y. Sun, *J. Coord. Chem*., 2020, **73**, 2728-2739.

S16. J. Ru, Y.-X. Shi, S.-C. Fu, Q. Guo, L.-L. Li and Y.-L. Wang, *Inorganica Chim. Acta*., 2023, **555**, 121574.

S17. X.-S. Wang, L. Li, D.-Q. Yuan, Y.-B. Huang and R. Cao, *J. Hazard. Mater*., 2018, **344**, 283-290.

S18. Y.-X. Shi, F.-L. Hu, F.-L. Hu and J.-P. Lang, *CrystEngComm*, 2015, **17**, 9404.

S19. Z. Xu, M. Su, X. He, B. Zhang, Y. Wang and H. Li, *Inorg. Chem. Commun*., 2020, **111**, 107644.

S20. A. Ma, J. Wu, Y. Han, F. Chen, B. Li, S. Cai, H. Huang, A. Singh, A. Kumar and J. Liu, *Dalton Trans.,* 2018, **47**, 9627.

S21. J. R. Lakowicz, *Principles of Fluorescence spectroscopy, 3rd ed., Springer, Singapore*, 2010, 443-472.

****